Synthesis and luminescence properties of cyclometalated iridium(III) complexes incorporating conjugated benzotriazole units

*Emily E. Langdon-Jones, Benjamin D. Ward, Simon J.A. Pope**

School of Chemistry, Main Building, Cardiff University,

Park Place, Cardiff, CF10 3AT, United Kingdom.

Abstract

The stepwise synthesis of imidazo[4,5-*f*]-1,10-phenanthroline-based ligands that incorporate conjugated benzotriazole units are described. Corresponding cyclometalated Ir(III) complexes of the type $[Ir(C^N)_2(L)]BF_4$ (where C^N = cyclometalating ligand; L = phenanthroline type ligand) are reported. The complexes were characterized using a variety of techniques, including IR, NMR, UV-vis. spectroscopies, mass spectrometry and cyclic voltammetry. The $[Ir(ppy)_2(L)]BF_4$ complexes display luminescence in the visible region with the benzotriazole variants showing long-lived blue shifted emission around 495 nm. Supporting TD-DFT calculations predict that a mixture of MLCT and LLCT character may contribute to the HOMO-LUMO transition of the benzotriazole derivatives.

Introduction

Cyclometalated Ir(III) complexes that possess luminescent properties have attracted significant attention [1] [1] since their initial discovery. Ir(III) complexes can be developed for a range of optoelectronic applications, such as OLEDs,[2] [2] light emitting electrochemical cells (LECs),[3][3] photoredox catalysts,[4][4] photovoltaics[5][5] and luminescence biomaging.[6][6] More recently, further applications of this class of compound have included piezochromics[7] [7] and responsive materials for data recording.[8][8] In all cases an understanding and control of the electronic properties of the complex are a prerequisite to its effective application. The aims of this work were to consider the use of substituted imidazo[4,5-*f*]-1,10-phenanthroline[9][9] species in the synthesis of conjugated benzotriazole-based Ir(III) species and to investigate the resultant luminescence properties.

Benzotriazoles are a very well-known class of aromatic heterocycle that contain three adjacently bonded nitrogen atoms. From a synthetic perspective, they are of interest because of their broad applicability, for example, in anti-corrosion[10] [10] products and for their diverse biological activity[11][11] (benzotriazoles are important drug precursors in the pharmaceutical industry). Interestingly, benzotriazoles can exhibit fluorescence emission and can also participate in coordination of metal ions *via* one or more of the nitrogen atoms making them attractive candidates in the design of larger polymetallic structures and coordination polymers.[12][12] The synthesis of benzotriazoles commonly (although myriad variants on the general approach are known)[13] relies upon the cycloaddition of potentially hazardous azide species with functionalized alkynes, often requiring metal-catalysed mediation.[14][14]

There are few examples of phosphorescent transition metal complexes that

incorporate the benzotriazole moiety.[15][15] Recently Choi *et al*. described a Re(I)-based species that incorporates a 1*H*-[1,2,3]triazolo[4,5-*c*]pyridine ligand (obtained *via* a 4,5-diaminopyridine ligand) which resulted in luminescence from the complex.[16][16] An Ir(III) complex that incorporates a benzotriazole moiety following reactivity with nitric oxide.[17][17]

Herein we describe the development of new *N*-alkyl-4-(1-phenyl-1*H*-imidazo[4,5-*f*][1,10]phenanthrolin-2-yl)benzene-1,2-diamine ligand scaffolds together with the synthesis and characterization of the corresponding $[Ir(N^C)_2(N^N)]BF_4$ complexes. Reaction with nitric oxide in solution allows facile formation of functionalized, conjugated benzotriazole derivatives that give modulated luminescence properties when incorporated into organometallic Ir(III) complexes.

Results and Discussion

Synthesis and Characterisation of $L^1 – L^4$

The adopted general synthetic route to the target benzotriazoles is shown in Scheme 1, where the addition of the -NHR' group provides control over the solubility properties.

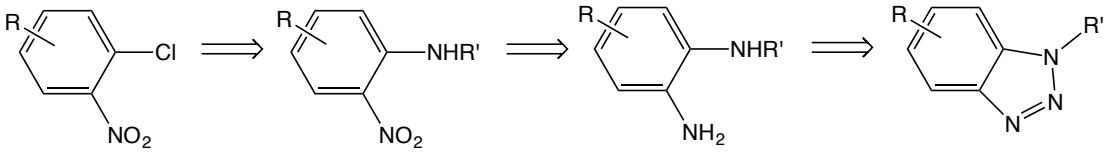

Scheme 1. General scheme showing the synthetic route to the benzotriazole species.

The nitro-substituted ligands ($\mathbf{L^1}$, $\mathbf{L^2}$) were synthesized from 1,10-phenanthroline-5,6-dione (Scheme 2) using 4-chloro-3-nitrobenzaldehyde, aniline and ammonium acetate in acetic acid to give the pro-ligand (top right, Scheme 2).[18,19] [18, 19] Further functionalization was achieved by heating the pro-ligand with either 2-(2-aminoethyl)ethanol or 3-aminopropanol in DMSO,[20] [20] to give the nitro-derived ligands, $\mathbf{L^1}$ and $\mathbf{L^2}$, respectively. These species were soluble in a range of common organic solvents.

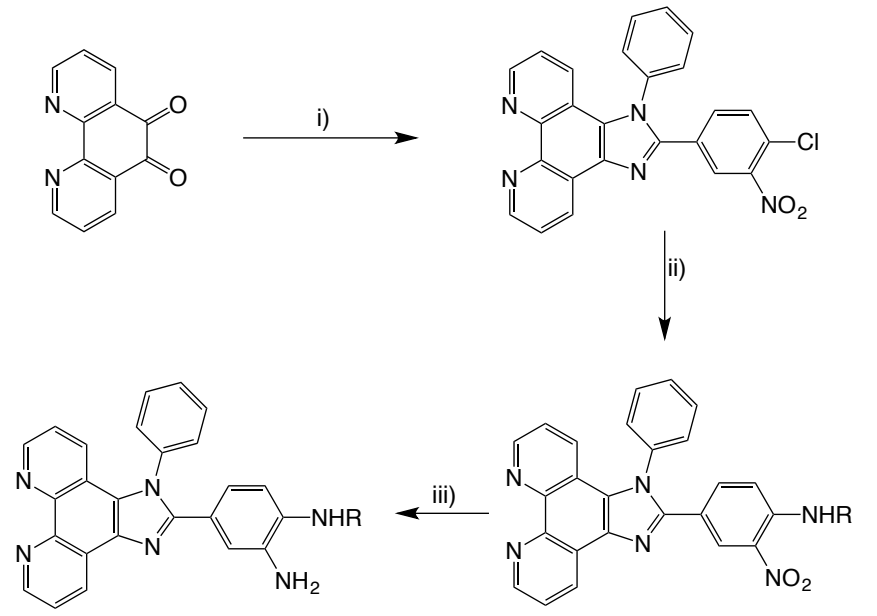

L[3] where R = $(CH_2)_2O(CH_2)_2OH$ **L**[1] where R = $(CH_2)_2O(CH_2)_2OH$

L[4] where R = $(CH_2)_3OH$ **L**[2] where R = $(CH_2)_3OH$

Scheme 2. Molecular structures and synthetic pathway to the ligands: (i) 4-chloro-3-nitrobenzaldehyde, NH_4OAc, glacial acetic acid; (ii) 2-(2-aminoethyl)ethanol or 3-aminopropanol, DMSO; (iii) H_2, Pd/C, methanol.

The completion of the aromatic substitution reaction was indicated through ^1H NMR spectroscopy by an upfield chemical shift (to 6.6–6.8 ppm) of the proton resonance (doublet) adjacent to the new aromatic amine substituent (Fig. S1). $^{13}C\{^1H\}$ NMR spectra were also consistent with the proposed structures for **L**[1] and **L**[2] and HRMS (ES^+) showed the presence of $[M+H]^+$ in both cases. Furthermore, the IR spectra revealed N*H* (*ca*. 3360 and 2920 cm^{-1}) and -NO_2 (*ca*. 1560 and 1360 cm^{-1}) vibrations consistent with the mixed amine/nitro aromatic substituents. Reduction of the nitro derivatives using standard conditions (H_2/Pd/C) correspondingly gave the diamino-adducts **L**[3] and **L**[4]. Again, ^1H (Fig. S1), $^{13}C\{^1H\}$ NMR and IR spectroscopies,

together with mass spectrometry, were used to confirm the formation of these new ligands.

Synthesis and Characterisation of Ir(III) complexes based on $L^1 – L^4$

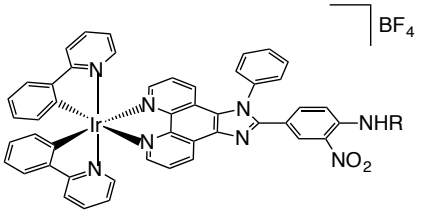

$[Ir(ppy)_2(L^{1-2})]BF_4$

L^1 where R = $(CH_2)_2O(CH_2)_2OH$

L^2 where R = $(CH_2)_3OH$

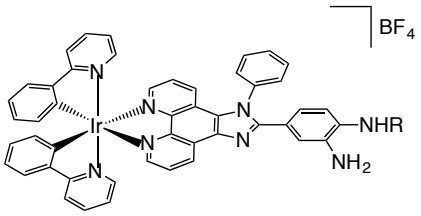

$[Ir(ppy)_2(L^{3-4})]BF_4$

L^3 where R = $(CH_2)_2O(CH_2)_2OH$

L^4 where R = $(CH_2)_3OH$

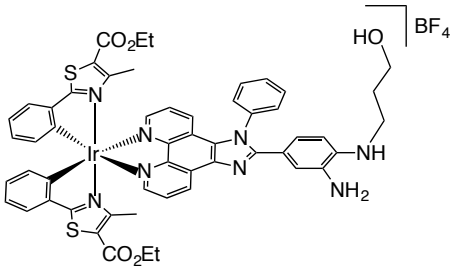

$[Ir(emptz)_2(L^4)]BF_4$

Scheme 3. Molecular structures of the isolated Ir(III) complexes based on $L^1 – L^4$.

For the initial series of Ir(III) complexes, the well-known $[Ir(ppy)_2(N^N)]BF_4$ (where ppy = 2-phenylpyridine; N^N = a diimine ligand) motif [21] [21] was targeted. The synthesis employed the intermediate bis–acetonitrile complex $[Ir(ppy)_2(MeCN)_2]BF_4$,[22] [22] which was then reacted with L^1-L^4 to give the corresponding complexes (Scheme 3) $[Ir(ppy)_2(L^{1-4})]BF_4$. For comparison, an alternative cyclometalating unit (emptz = ethyl-4-methyl-2-phenylthiazole-5-

carboxylate) [23] [23] was also utilized and thus $[Ir(emptz)_2(\mathbf{L^4})]BF_4$ was also synthesized using the same method described above for the ppy analogue.

All new complexes were characterized using a range of spectroscopic techniques and the data are collected in the Experimental section. The ^1H NMR spectra of the complexes show aromatic regions with overlapping resonances associated with the cyclometalated and diimine ligands (e.g. Fig. S2, SI). For $[Ir(emptz)_2(\mathbf{L^4})]BF_4$, the retention of the ethyl ester functionality was clearly observed in the aliphatic region of the spectrum. IR spectroscopy also highlighted the ester functionality of the emptz species (*ca*. 1710 cm^{-1}) and the BF_4^- counter ion stretches at *ca.* 1160 and 1030 cm^{-1}. High resolution mass spectra were obtained for all complexes revealing the parent cations of $[M - BF_4]^+$ with the appropriate isotopic distribution for iridium in each case (Fig. S3, SI).

Synthesis and characterisation of benzotriazole derivatives

The benzotriazole derivatives of selected ligands and complexes were synthesized using the 1,2-diamine derivatives $\mathbf{L^{3/4}}$, $[Ir(ppy)_2(\mathbf{L^{3/4}})]BF_4$ and $[Ir(emptz)_2(\mathbf{L^4})]BF_4$ (Scheme 3). The diamino derivative was dissolved in de-aerated chloroform and NO gas was bubbled into the reaction vessel. An indication of reaction was immediate, with a rapid color change of the reaction medium. The solution was then exposed to air and after work-up (see Experimental section for details) the benzotriazole products $\mathbf{L^{5/6}}$ (Scheme 4), $[Ir(ppy)_2(\mathbf{L^{5/6}})]BF_4$ and $[Ir(emptz)_2(\mathbf{L^6})]BF_4$, were isolated in moderate-to-high yields and fully characterized.

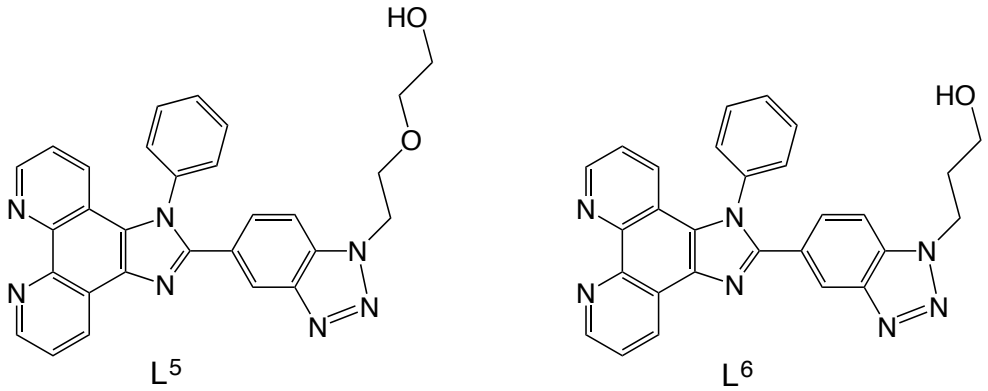

Scheme 4. Structures of the benzotriazole derived ligands $\mathbf{L^5}$ and $\mathbf{L^6}$.

In all cases, ^{1}H NMR spectroscopy showed the loss of the key N*H* resonance in all cases, and significant downfield shifts [24][24] (*ca*. 0.4–1.0 ppm) of the aromatic resonances, which are attributed to transformation to the benzotriazole group. Both low and high resolution mass spectra showed the presence of $[M–BF_4]^+$ for $[Ir(ppy)_2(\mathbf{L^{5/6}})]BF_4$ and $[Ir(emptz)_2(\mathbf{L^6})]BF_4$. IR spectroscopic studies on $\mathbf{L^{5/6}}$ and the corresponding complexes showed a new peak *ca*. 1330 cm^{-1}, which was assigned to the presence of the triazole moiety.

Electrochemistry of the complexes

The electrochemical characteristics of the complexes were studied in de-oxygenated acetonitrile (Table 1). The cyclic voltammograms were measured at a platinum disc electrode (scan rate υ = 200 mVs^{-1}, 10^{-3} M solutions, 0.1 M $[NBu_4][PF_6]$ as a supporting electrolyte) using the couple of $[Fe(\eta\text{-}C_5H_5)_2]^{0/1+}$ as an internal reference.

Table 1. Electrochemical properties of the complexes.

Complex	E_{ox} / V[a]	E_{red} / V[a]	HOMO / eV[c]
$[Ir(ppy)_2(\mathbf{L^1})]BF_4$	+1.35[b]	–1.13,[b] –1.42[b]	-5.69
$[Ir(ppy)_2(\mathbf{L^2})]BF_4$	+1.36[b]	–1.23,[b] –1.47[b]	-5.70
$[Ir(ppy)_2(\mathbf{L^3})]BF_4$	+1.36[b]	–1.42	-5.70
$[Ir(ppy)_2(\mathbf{L^4})]BF_4$	+1.40[b]	–1.38	-5.74
$[Ir(ppy)_2(\mathbf{L^5})]BF_4$	+1.35[b]	–1.42[b]	-5.69
$[Ir(ppy)_2(\mathbf{L^6})]BF_4$	+1.78[b]	–1.30,[b] –1.46[b]	-6.12
$[Ir(emptz)_2(\mathbf{L^4})]BF_4$	+1.51[b]	–1.37,[b] –1.65[b]	-5.85
$[Ir(emptz)_2(\mathbf{L^6})]BF_4$	+1.42[b]	–1.40[b]	-5.76

[a] measured as dichloromethane solutions at 200 mVs^{-1} with 0.1 M $[NBu_4][PF_6]$ as supporting electrolyte calibrated with Fc/Fc^+; [b] irreversible oxidations and reductions are reported as anodic and cathodic peak potentials, respectively; [c] the HOMO energy level was calculated using the equation $-E_{HOMO}$ (eV) = $E_{ox} - E_{Fc/Fc^+} + 4.8$.

Each complex showed one non–fully reversible oxidation, generally over the range +1.35 to +1.51 V, assigned to the $Ir^{3+/4+}$ couple.[25][25] The oxidation potential of the complexes containing the glycol appended ligands ($\mathbf{L^1}$, $\mathbf{L^3}$ and $\mathbf{L^5}$) was invariant across the series. On the other hand, for the $[Ir(ppy)_2(\mathbf{L^{2/4/6}})]BF_4$ group of complexes the benzotriazole derivative gave the highest E_{ox} value. Comparison of ppy and emptz derivatives also showed subtle changes in the value of the $Ir^{3+/4+}$ oxidative couple. Each complex generally showed irreversible features on the reduction wave, with one or two features –1.37 to –1.47 V. Only the diamino-derived complexes $[Ir(ppy)_2(\mathbf{L^3})]BF_4$ and $[Ir(ppy)_2(\mathbf{L^3})]BF_4$ showed reversible reductions. These were assigned as ligand–centred processes involving both the diimine and/or the

cyclometalating ligands. Related imidazo[4,5-*f*]-1,10-phenanthroline examples in the literature by Jayabharathi *et al* [26][26] have shown reversible reduction waves at *ca*. –1.76 and –2.00 V, respectively. The complexes $[Ir(ppy)_2(\mathbf{L^1})]BF_4$ and $[Ir(ppy)_2(\mathbf{L^1})]BF_4$ show two irreversible reduction features, one of which is attributed to the presence of the nitro-functionalised phenyl group appended to the imidazo[4,5-*f*]-1,10-phenanthroline, the other is likely due to the ppy ligands.

DFT calculations

To probe the predicted nature of the electronic transitions involved in these systems, calculated representative ligand and complex structures and modelled excited state energies using DFT and TD-DFT respectively. To reduce the computational complexity, the calculations made use of a simplified model compound that incorporated a methylamine substituent, ($\mathbf{L^{Me1}}$) and the corresponding N-methyl substituted benzotriazole ($\mathbf{L^{Me2}}$) (Scheme 5); these simplifications are expected to have a relatively minor effect on the excited state energies, which are likely to be dominated by significant π–π* and charge transfer transitions. Solvation (using MeCN) was included in all calculations to imitate the experimental conditions as closely as possible.

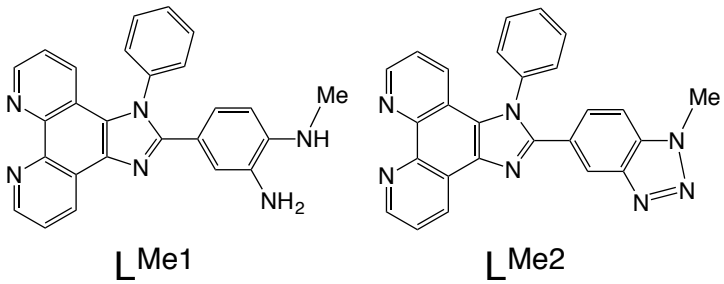

Scheme 5. Model ligands used for the DFT and TD-DFT calculations.

In each case, the first 50 excited states were modelled to ensure all transitions down to *ca*. 200 nm were considered; details of the excitation energies are provided in the SI. Simulated absorption spectra of $\mathbf{L^{Me1}}$ and $\mathbf{L^{Me2}}$ are provided in Fig. 1, along with isosurfaces depicting the HOMOs and LUMOs obtained from the calculations. In these studies, TD–DFT calculations employing the B3LYP[27] [27] or M06[28] [28] functionals substantially overestimated the excitation wavelengths by an additional *ca.* 50 nm;[29] [29] the long range corrected hybrid exchange correlation functional CAM-B3LYP [29][36] was therefore employed to give an improved description of excited states in systems where there is a significant charge transfer component. The use of CAM-B3LYP gave excited state energies that were in closer agreement with the experimental data. The electronic properties of the corresponding iridium(III) complexes bearing these model ligands ($\mathbf{L^{Me1/2}}$) were also probed using the same level of theory as the uncoordinated ligands.

For both $\mathbf{L^{Me1}}$ and $\mathbf{L^{Me2}}$, TD–DFT studies predict a π–π* assignment of the lowest lying absorption bands involving a HOMO to LUMO transition with predicted maxima at 305 and 300 nm, respectively. The HOMO for $\mathbf{L^{Me1}}$ is associated with the majority of the π-system (all except for the out-of-plane phenyl ring), whereas the LUMO was predominantly associated with the imidazo–phenanthroline core. This contrasts with the benzotriazole variant, $\mathbf{L^{Me2}}$, where the LUMO was mostly situated on the N-phenylimidazo and benzotriazole moieties. For both $\mathbf{L^{Me1}}$ and $\mathbf{L^{Me2}}$ a set of stronger bands between 240–290 nm, were also predicted to have both π–π* transitions and intramolecular charge transfer (ICT) contributions. The calculations predicted a hypsochromic shift upon formation of the benzotriazole (Fig. 1).

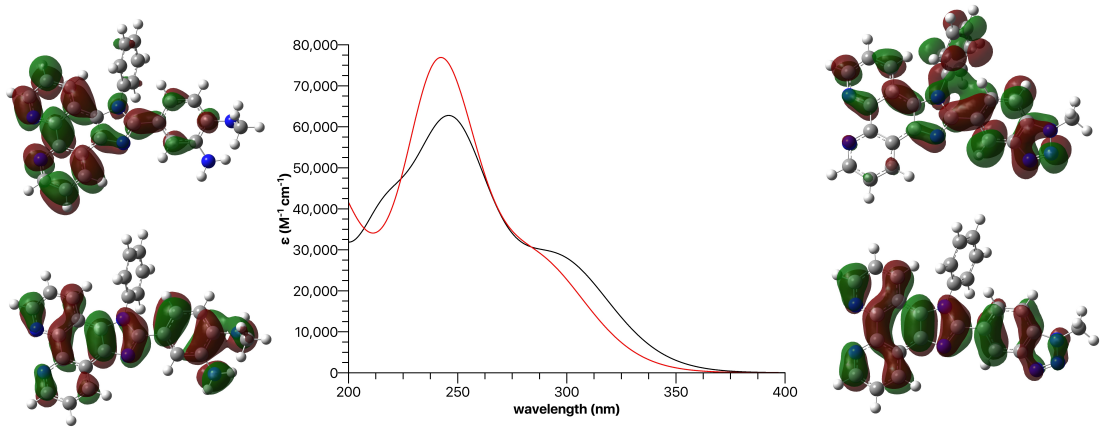

Figure 1. Simulated UV-vis absorption spectra[30][30] (centre) of $\mathbf{L}^{\mathbf{Me1}}$ (solid) and $\mathbf{L}^{\mathbf{Me2}}$ (dotted), alongside depictions of the calculated frontier orbitals (LUMO, top; HOMO, bottom) for $\mathbf{L}^{\mathbf{Me1}}$ (left) and $\mathbf{L}^{\mathbf{Me2}}$ (right). Hydrogen atoms omitted for clarity.

TD–DFT calculations on $[Ir(ppy)_2(\mathbf{L}^{\mathbf{Me1/2}})]^+$ (Fig. 2) suggest a substantial mixing of MLCT and LLCT/ILCT character to the lowest lying absorption bands.[31][31] Figure 2 shows very clear differences in the predicted nature of the HOMO and HOMO–1 for each complex, both of which are involved in these bands. For the diamino derivative $[Ir(ppy)_2(\mathbf{L}^{\mathbf{Me1}})]^+$, the lowest energy band of substantial intensity (339 nm) corresponds to the HOMO→LUMO transition; the HOMO is localized exclusively over the terminal diaminophenylene moiety thus predicting a much stronger ILCT character to the HOMO-LUMO band.

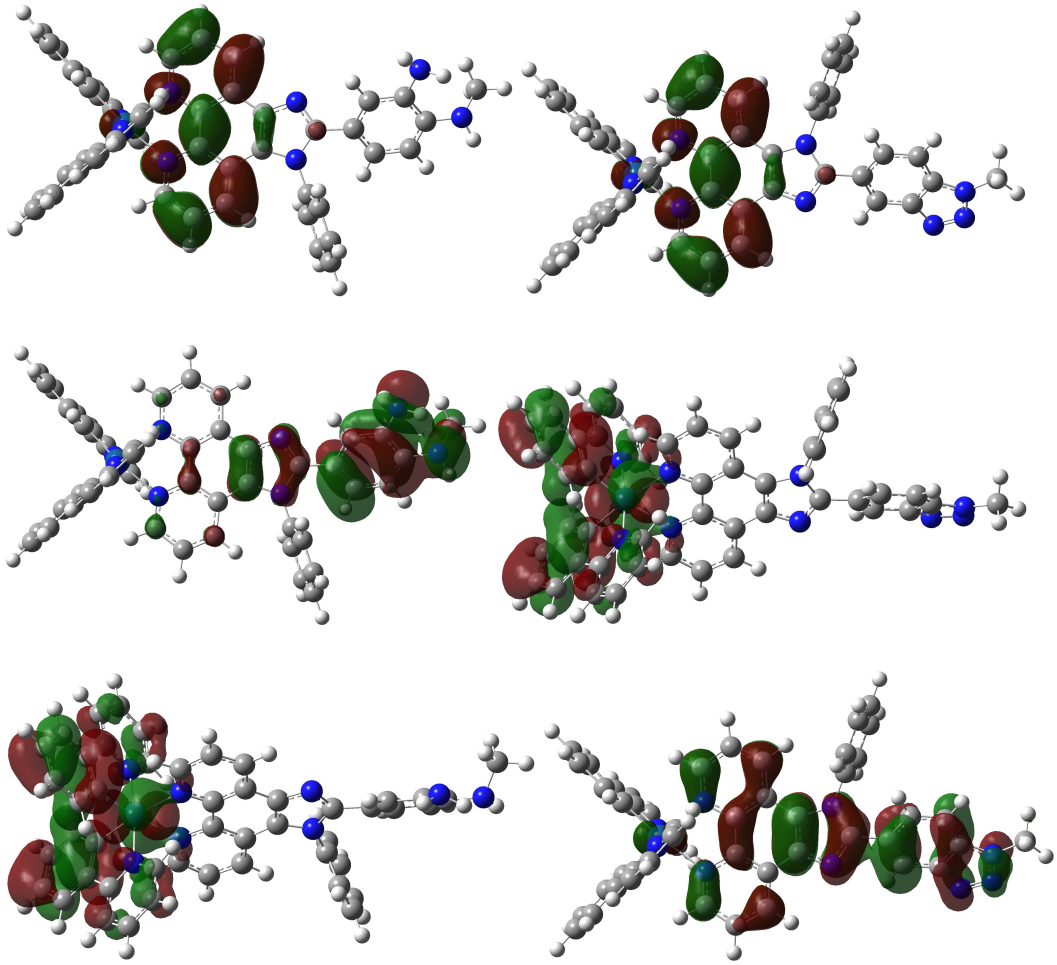

Figure 2. Calculated frontier orbitals (LUMO, top; HOMO, middle; HOMO–1, bottom) of the model complexes $[Ir(ppy)_2(L^{Me1})]^+$ (left) and $[Ir(ppy)_2(L^{Me2})]^+$ (right). Hydrogen atoms omitted for clarity.

Calculations on the benzotriazole derivative $[Ir(ppy)_2(\mathbf{L^{Me2}})]^+$ predict a very different nature to the corresponding lowest energy transition of appreciable intensity at 329 nm, which arises from a HOMO–1→LUMO transition. Although this is a different transition to that for $[Ir(ppy)_2(\mathbf{L^{Me1}})]^+$, the nature of the transition is comparable, being predominantly $\pi\rightarrow\pi^*$ in character; the HOMO–1 has a comparable set of orbital coefficients over the benzotriazole moiety, but is now much more delocalized, compared to that in $[Ir(ppy)_2(\mathbf{L^{Me1}})]^+$, thereby corresponding to a lower energy orbital. A further transition, dominated by excitation from the (Ir-5*d* + ppy-π) orbitals

(HOMO–1 in $[Ir(ppy)_2(\mathbf{L}^{\mathbf{Me1}})]^+$ and HOMO in $[Ir(ppy)_2(\mathbf{L}^{\mathbf{Me2}})]^+$) to LUMO (phenanthroline-π^*), is effectively unchanged at 326 nm. The simulated (MeCN) UV-vis. spectra of $Ir(ppy)_2(\mathbf{L}^{\mathbf{Me1/2}})]^+$ are shown in the SI (Fig. S4) and predict *ca*. 15 nm hypsochromic shift upon formation of the benzotriazole species. An analysis of the orbital energies of interest to this study shows that the LUMO energies are largely unaltered between $[Ir(ppy)_2(\mathbf{L}^{\mathbf{Me1}})]^+$ (–1.33 eV) and $[Ir(ppy)_2(\mathbf{L}^{\mathbf{Me2}})]^+$ (–1.34 eV), whereas the HOMO energies show a substantial difference (–6.86 eV for $[Ir(ppy)_2(\mathbf{L}^{\mathbf{Me1}})]^+$ and –7.14 eV for $[Ir(ppy)_2(\mathbf{L}^{\mathbf{Me2}})]^+$); the difference in HOMO energies is in good agreement with those obtained in the electrochemical analyses, above. Further analysis indicates that the HOMO–1 in $[Ir(ppy)_2(\mathbf{L}^{\mathbf{Me1}})]^+$ has an almost identical energy to the HOMO in $[Ir(ppy)_2(\mathbf{L}^{\mathbf{Me2}})]^+$ (–7.14 eV for each); these orbitals are moreover essentially identical in appearance. It therefore appears that the HOMO in $[Ir(ppy)_2(\mathbf{L}^{\mathbf{Me1}})]^+$, which is based primarily over the terminal diaminophenylene, is lowered in energy upon reaction with NO, presumably as a result of greater delocalization, so that is lies below the (Ir-5*d* + ppy-π) orbital; this HOMO–1 orbital therefore becomes the HOMO in $[Ir(ppy)_2(\mathbf{L}^{\mathbf{Me2}})]^+$, even though its energy is unaffected. The orbital in $[Ir(ppy)_2(\mathbf{L}^{\mathbf{Me2}})]^+$ that most closely resembles the HOMO from $[Ir(ppy)_2(\mathbf{L}^{\mathbf{Me1}})]^+$ is the HOMO-1 (*e.g*. in terms of orbital phases and the location of the nodes over the benzotriazole component); this correlates well with the expected transitions calculated in the TD-DFT studies above.

Electronic properties of the ligands and Ir(III) complexes

The UV-vis. absorption spectra of the ligands were recorded in aerated MeCN (2.5×10^{-5} M) (Fig. 3). All ligands possessed strong absorption bands <400 nm, assigned to overlapping spin-allowed π–π^* and imidazole–based n–π^* transitions. The wavelength positioning of the lowest energy bands for $\mathbf{L}^{\mathbf{3/4}}$ are in quite good

agreement with the TD-DFT calculations. The spectra of the nitro derivatives ($\mathbf{L}^{1/2}$) also showed a weak, broad band *ca*. 450 nm that is tentatively assigned to an intramolecular charge transfer (ICT) transition localized on the ligand.

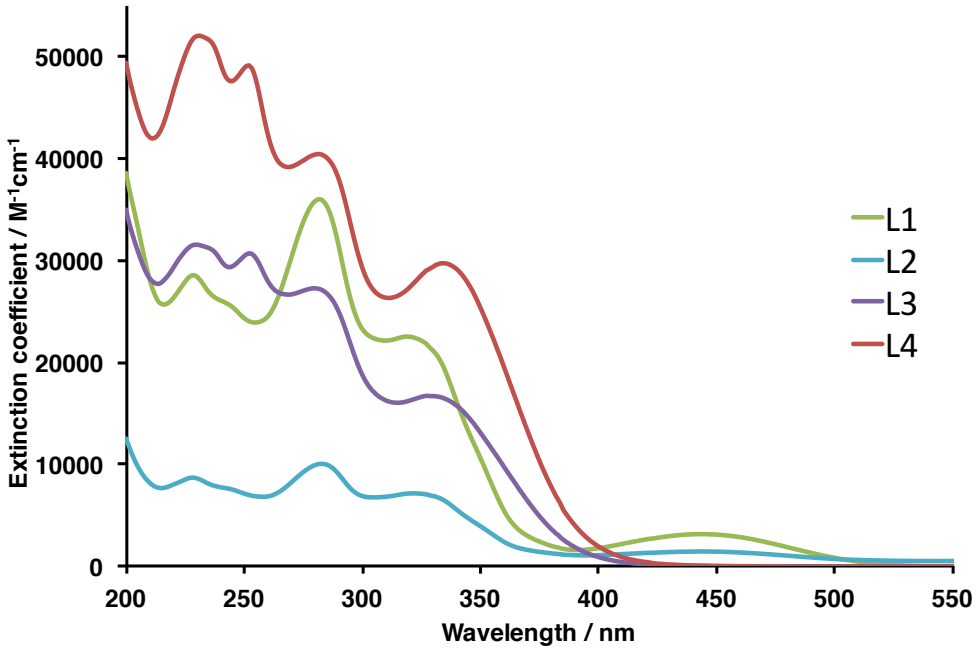

Figure 3. UV-vis absorption profiles of the ligands (MeCN, 2.5×10^{-5} M).

The UV-vis. spectra of the iridium(III) complexes (e.g. Fig. 4) can largely be described as comprising metal–perturbed, ligand–centred[32] [32] absorption bands between 200–380 nm, and a set of weaker bands in the visible region at 350–500 nm. These latter bands were assigned to overlapping spin-allowed ^{1}MLCT (Ir(*d*)–π^*) and ^{1}ILCT (π_{phenyl}–$\pi^*_{imidazo}$) transitions,[33] [33] with the possibility of spin–forbidden ^{3}MLCT transitions contributing to the weaker, low-energy shoulder towards 500 nm. Variation of the coordinated diimine ligand resulted in minor tuning of the absorption bands, whilst changing the cyclometalating unit from ppy to emptz resulted in a more pronounced MLCT feature *ca*. 450 nm for the latter.

The electronic properties of the benzotriazole-derived ligands ($\mathbf{L}^{5/6}$) showed a 5–20 nm hypsochromic shift of the absorption bands relative to their diamino precursors, consistent with the predictions from TD-DFT (10 nm shift of the lowest energy band of significant intensity). Figure 5 shows that formation of the benzotriazole complex derivative induced shifts in both ^{1}MLCT and ligand-centered transitions throughout the UV-vis regions. The observed trend was a hypsochromic shift in the lowest lying absorption band of the complexes after formation of the benzotriazole species.

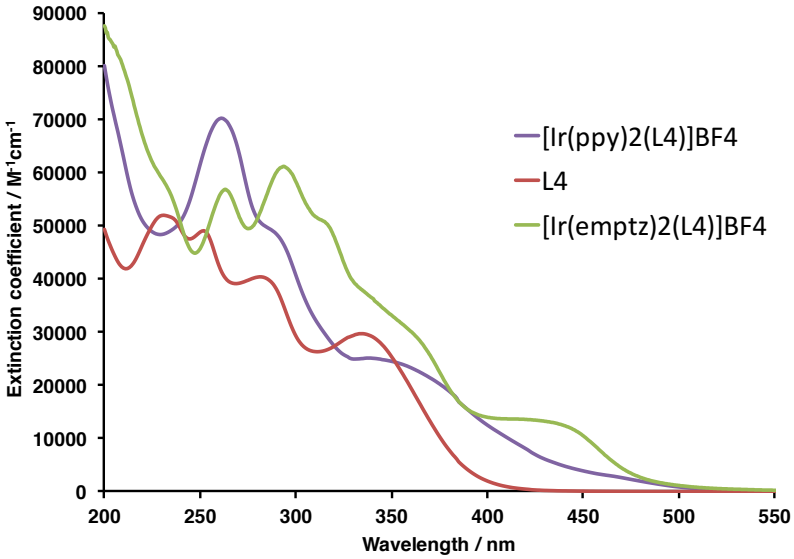

Figure 4. UV-vis absorption spectra of $\mathbf{L}^{4}$, [Ir(ppy)$_2$($\mathbf{L}^{4}$)]BF$_4$ and [Ir(emptz)$_2$($\mathbf{L}^{4}$)]BF$_4$ in MeCN at 2.5 × 10^{-5} M.

The luminescence properties of all ligands and complexes were measured in aerated MeCN (Table 2).

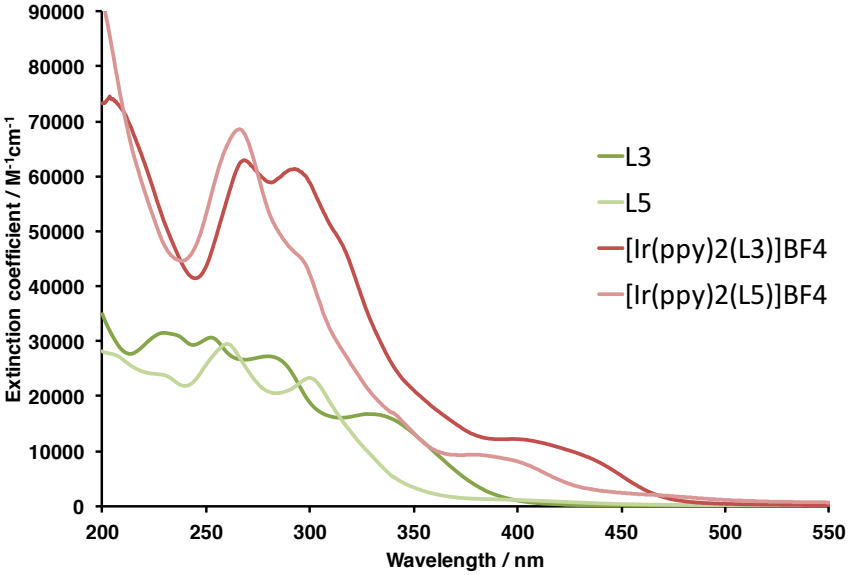

Figure 5. UV-vis absorption spectra of $\mathbf{L^3}$, $\mathbf{L^5}$, $[Ir(ppy)_2(\mathbf{L^3})]BF_4$ and $[Ir(ppy)_2(\mathbf{L^5})]BF_4$ in MeCN at 2.5×10^{-5} M.

Table 2. Absorption and emission properties of the complexes.

Compound	λ_{abs} / nm[a]	λ_{em} / nm[a,b,c]	τ / ns[a,d]	Φ[a,e]
$[Ir(ppy)_2(\mathbf{L^1})]BF_4$	455 sh, 412, 318 sh, 290 sh, 269	522 (433)	7, 17 (80 %)	0.01
$[Ir(ppy)_2(\mathbf{L^2})]BF_4$	456 sh, 414 sh, 316 sh, 293 sh, 269	517 (427)	21	0.01
$[Ir(ppy)_2(\mathbf{L^3})]BF_4$	433 sh, 403, 315 sh, 292, 268	579 (431)	5, 65 (92 %)	0.02
$[Ir(ppy)_2(\mathbf{L^4})]BF_4$	466 sh, 410 sh, 344, 288 sh	579 (435)	63	0.02
$[Ir(ppy)_2(\mathbf{L^5})]BF_4$	463 sh, 382, 341 sh, 293 sh, 266	510 (418)	9, 70 (78 %)	0.05
$[Ir(ppy)_2(\mathbf{L^6})]BF_4$	392 sh, 342 sh, 287 sh, 263	496 (416)	320	0.02
$[Ir(emptz)_2(\mathbf{L^4})]BF_4$	418 sh, 355 sh, 316 sh, 294, 262	548 (435)	239	0.01
$[Ir(emptz)_2(\mathbf{L^6})]BF_4$	403 sh, 355 sh, 313 sh, 293, 268	546 (416)	322	0.11

[a] recorded in aerated MeCN solution; [b] free ligand values in parentheses; [c] λ_{exc} = 355 nm; [d] λ_{exc} = 372 nm; [e] using $[Ru(bpy)_3](PF_6)_2$ in aerated MeCN as a standard (Φ_{em} = 0.016)

Room temperature solution state (aerated MeCN) luminescence data showed that all ligands were emissive. Upon irradiation at 355 nm ligands produced a broad emission

band between 416-435 nm, which is characteristic of phenylimidazo–phenanthroline ligands of this type.[39][39] The emission lifetimes (Table 2) of the ligands were indicative of a fluorescence ($^1\pi$–π*) in all cases, with lifetimes <5 ns. It is notable that in the series, the pair of benzotriazole derivatives ($\mathbf{L}^{5/6}$) have the shortest wavelength emission, revealing a clear distinction from their diamino counterparts ($\mathbf{L}^{3/4}$).

Room temperature luminescence measurements on aerated MeCN solutions of the complexes (Table 2 and Fig. 6) showed visible green or orange emission in the range 490–580 nm. For the ppy complexes, highly tuneable emission wavelengths were observed between the nitro- (λ_{em} ~ 520 nm), diamino- (λ_{em} ~ 580 nm) and benzotriazole-functionalized (λ_{em} ~ 495 nm) complexes. The comparison of $[Ir(ppy)_2(\mathbf{L}^4)]BF_4$ and $[Ir(emptz)_2(\mathbf{L}^4)]BF_4$ revealed a much stronger vibronic component to the emission band of the latter, as observed previously.[23]

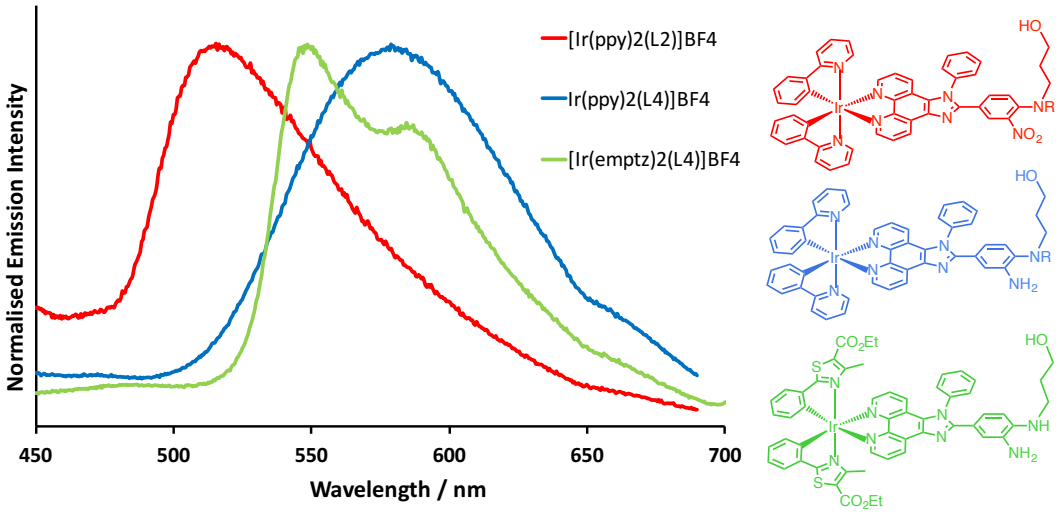

Figure 6. Comparison of the emission spectra of selected complexes recorded in aerated MeCN.

Time–resolved emission measurements revealed that the lifetimes varied across the series of complexes. Lifetimes for $[Ir(ppy)_2(\mathbf{L})]BF_4$ species were observed between 20–65 ns, which are significantly shorter than generally observed for cyclometalated Ir(III) complexes.[34][34] This suggests that some degree of excited state quenching is operative in these complexes, possibly due to the presence of both amine and nitro groups. Further support for this was indicated by the relatively low quantum yield values (typically between 0.5–5%). The shortest lifetime values (*ca*. 20 ns) were observed for complexes of the nitro-functionalized ligands, suggesting that the nitro group acts as an effective excited state quencher in these systems. Again, the nitro-derived species showed the lowest quantum yield values consistent with a quenching phenomenon. In comparison, the recorded lifetime for $[Ir(emptz)_2(\mathbf{L}^4)]BF_4$ was 239 ns and much more comparable to previous studies,[23] indicating much less sensitivity to quenching for this structural variant.

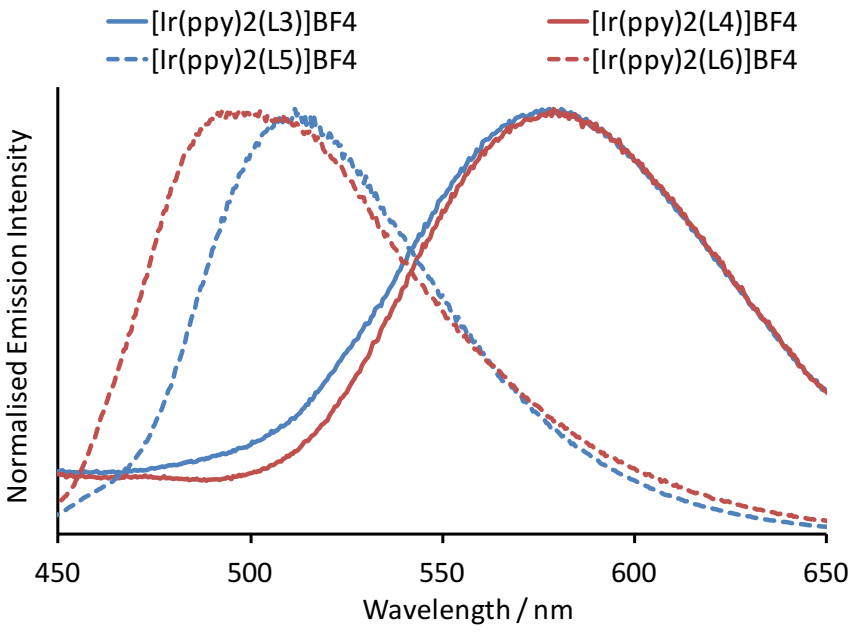

Figure 7. Comparison of the emission spectra of selected diamino-derived complexes and the related benzotriazole species (recorded in aerated MeCN).

The corresponding luminescence properties of the benzotriazole complexes $[Ir(ppy)_2(\mathbf{L}^{5/6})]BF_4$ showed a large hypsochromic shift relative to the corresponding diamino-analogues (Fig. 7). In contrast, whilst little shift of the emission wavelength was observed between $[Ir(emptz)_2(\mathbf{L}^{4/6})]BF_4$, analysis of the integrated emission intensity showed a 10–fold enhancement upon formation of the benzotriazole derivative (Fig. 8). This luminescence enhancement was further supported by quantum yield measurements that showed an increase to 11%, and a lengthening of the phosphorescence lifetime from 239 to 322 ns. Taken together this suggests that formation of the benzotriazole derivative reduces quenching pathways from the triplet emitting state. Previous studies on organic fluorophores have suggested that this enhancement is due to the removal of a *o*–phenylenediamine unit that can act as an efficient quencher of excited states *via* photoinduced electron transfer.[15][15]

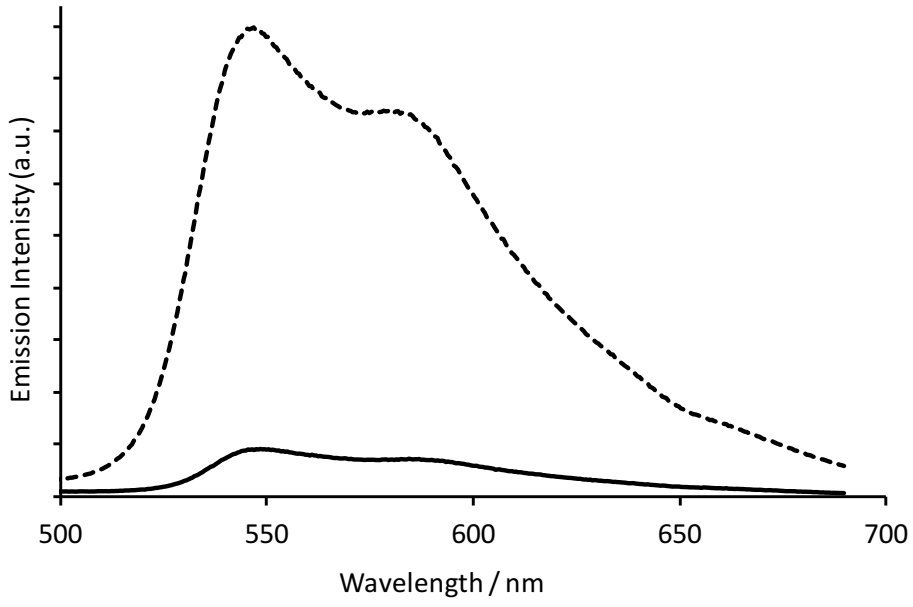

Figure 8. Comparison of emission spectra of $[Ir(emptz)_2(\mathbf{L}^4)]BF_4$ (solid) and $[Ir(emptz)_2(\mathbf{L}^6)]BF_4$ (dashed) (recorded in aerated MeCN).

In summary, diimine type ligands based on substituted imidazo[4,5-*f*]-1,10-phenanthroline can be suitably functionalized to yield conjugated new benzotriazole derivatives. These species can be utilized as an ancillary ligand in corresponding cyclometalated Ir(III) complexes of the form $[Ir(C^N)_2(L)]^+$. The complexes display visible luminescence in solution, which can either be modulated or enhanced by the presence of the benzotriazole group within the substituted imidazo[4,5-*f*]-1,10-phenanthroline.

Experimental

DFT Studies

Scalar relativistic DFT calculations were carried out using the Gaussian 09 package,[35] with relativistic effects incorporated *via* the use of appropriate effective core potentials (ECPs). Geometry optimizations were performed without symmetry constraints at the CAM–B3LYP level,[36][36] which was developed specifically to improve the description of excited states involving substantial charge-transfer character. The D3 version of Grimme's dispersion correction was included in all calculations.[37][37] The calculations were undertaken with a basis set consisting of the Stuttgart-Dresden basis set plus ECP on Ir, and the cc–pVDZ double–ζ basis set on all remaining atoms.[38][38] Stationary points were analysed using frequency calculations, to ascertain that they were minima on the potential energy surface. Time-dependent DFT (TD–DFT) calculations also employed CAM–B3LYP; the first 50 excited states were calculated. As shown by Vlček *et al.*,[39][39] solvent effects can be crucial for

obtaining satisfactory agreement between experiment and TD–DFT. Solvent was therefore modelled using the polarizable continuum model,[40][40] with the molecular cavity defined by a united atom model that incorporates hydrogen into the parent heavy atom, and included in both geometry optimizations and TD-DFT calculations.

Electrochemical studies

Electrochemical studies were carried out using a Parstat 2273 potentiostat in conjunction with a three-electrode cell. The auxiliary electrode was a platinum wire and the working electrode a platinum (1.0 mm diameter) disc. The reference was a silver wire separated from the test solution by a fine porosity frit and an agar bridge saturated with KCl. Solutions (10 mL MeCN) were 10^{-3} M in the test compound and 0.1 M in $[NBuN_4][PF_6]$ as the supporting electrolyte. Under these conditions, $E^{0\prime}$ for the one electron oxidation of $[Fe(\eta\text{-}C_5H_5)_2]$, added to the test solutions as an internal calibrant, is 0.46 V. Unless specified, all electrochemical values are at υ = 200 mV s^{-1}.

General

^1H and $^{13}C\{^1H\}$ NMR spectra were recorded on an NMR–FT Bruker 400 MHz or Jeol Eclipse 300 MHz spectrometer and recorded in $CDCl_3$, CD_3CN or DMSO–d_6. ^1H and $^{13}C\{^1H\}$ NMR chemical shifts (δ) were determined relative to residual solvent peaks with digital locking and are given in ppm. Low–resolution mass spectra were obtained by the analytical services at Cardiff University. High–resolution mass spectra were carried out at the EPSRC National Mass Spectrometry Service at Swansea University. UV−vis studies were performed on a Jasco V–570 spectrophotometer in MeCN solutions (2.5×10^{-5} M). IR spectra were recorded on a Thermo Scientific Nicolet iS5

spectrometer fitted with an iD3 ATR attachment. Photophysical data were obtained on a JobinYvon−Horiba Fluorolog spectrometer fitted with a JY TBX picoseconds photodetection module. The pulsed source was a Nano-LED configured for 372 nm output operating at 1 MHz. Luminescence lifetime profiles were obtained using the JobinYvon−Horiba FluoroHub single photon counting module and the data fits yielded the lifetime values using the provided DAS6 deconvolution software. Quantum yield measurements were obtained on aerated MeCN solutions of the complexes, using $[Ru(bpy)_3](PF_6)_2$ in aerated MeCN as a standard ($\Phi_{em} = 0.016$).[41]

All reactions were performed with the use of vacuum line and Schlenk techniques. Reagents were commercial grade and were used without further purification. 1,10–Phenanthroline–5,6–dione was synthesized according to the literature.[42]

Synthesis

Synthesis of 2–(3'–nitro–4'–chlorophenyl)–1–phenyl–1H–imidazo[4,5-f][1,10]–phenanthroline

1,10–phenanthroline–5,6–dione (450 mg, 2.14 mmol), aniline (0.20 mL, 2.14 mmol), 4–chloro–3–nitrobenzaldehyde (397 mg, 2.14 mmol) and ammonium acetate (1.65 g, 21.4 mmol) in glacial acetic acid (9 mL) were heated at reflux for 3 hours. The cooled solution was poured into ice cold water (200 mL) and neutralized with 10 % NH_4OH solution. To this, one drop of 50 % hypochlorite solution was added and the yellow precipitate then extracted into CH_2Cl_2 (2 × 200 mL) and washed with water (2 × 200 mL). The organic phase was dried over $MgSO_4$ and the volume reduced to allow precipitation by the addition of Et_2O. The precipitate was filtered and dried to give the product as a yellow powder (yield = 787 mg, 81 %). ^{1}H NMR (400 MHz, $CDCl_3$): δ_H

= 9.16–9.12 (m, 1H), 9.07–9.01 (m, 2H), 8.04 (s, 1H, NO_2CCH), 7.74–7.62 (m, 5H, phenyl), 7.52 (d, 2H, $^3J_{HH}$ = 7.3 Hz), 7.49–7.37 (m, 2H), 7.27–7.20 (m, 1H) ppm.

Synthesis of ***L*^{1}**

2–(2–aminoethyl)ethanol (0.52 mL, 5.27 mmol) was added to 2–(3'–nitro–4'–chlorophenyl)–1–phenyl–1H–imidazo[4,5-*f*][1,10]–phenanthroline (426 mg, 1.05 mmol) and stirred in DMSO (6 mL) under a dinitrogen atmosphere. The slurry was heated at *ca.* 80 ºC for 48 hours then cooled, and the product precipitated by the addition of water (20 mL). The reaction mixture was then neutralized with 1M HCl and the product isolated by filtration. Washing with copious amounts of water and then oven drying gave **L^1** as an orange-red powder (yield = 378 mg, 69 %). ^{1}H NMR (400 MHz, $CDCl_3$): δ_H = 9.13–9.11 (m, 1H), 9.06 (dd, 1H, J_{HH} = 8.1, 8.3 Hz), 9.00–8.97 (m, 1H), 8.34 (broad t, 1H, $^3J_{HH}$ = 4.2 Hz, N*H*), 8.17 (s, 1H), 7.87 (dd, 1H, J_{HH} = 9.0, 6.1 Hz), 7.72–7.63 (m, 4H), 7.53 (d, 1H, $^3J_{HH}$ = 7.6 Hz), 7.52 (d, 1H, $^3J_{HH}$ = 8.1 Hz), 7.40 (dd, 1H, J_{HH} = 8.4 Hz), 7.24 (dd, 1H, J_{HH} = 8.4 Hz), 6.80 (d, 1H, $^3J_{HH}$ = 9.2 Hz), 3.76–3.70 (m, 4H, CH_2CH_2), 3.58 (t, 2H, $^3J_{HH}$ = 4.8 Hz, OCH_2CH_2), 3.47 (app. quar., 2H, $^3J_{HH}$ = 5.3 Hz, OCH_2CH_2), 1.87 (broad s, 1H, O*H*) ppm. $^{13}C\{^1H\}$ NMR (151 MHz, $CDCl_3$): δ_C = 150.3, 148.7, 148.0, 145.4, 137.8, 136.5, 135.9, 131.5, 131.0, 130.8, 128.6, 128.1, 127.2, 127.0, 123.9, 123.6, 122.5, 119.8, 117.1, 114.0, 72.5, 68.9, 61.9, 42.7 ppm. LRMS (AP^+) found *m/z* 521.19 for $[M+H]^+$; HRMS (ES^+) found *m/z* 521.1923, calculated at 521.1932 for $[C_{29}H_{24}N_6O_4+H]^+$. IR (solid) ν_{max}: 3356, 2922, 2858, 1627, 1597, 1571, 1517, 1496, 1469, 1446, 1390, 1354, 1286, 1255, 1224, 1184, 1151, 1118, 1060, 1028, 987, 960, 929, 887, 823, 798, 783, 736, 711, 677, 653, 615, 529, 488, 457, 424, 416, 407 cm^{-1}. UV-Vis (MeCN) λ_{max} ($\varepsilon/M^{-1}cm^{-1}$): 447 (3200), 322 (22400), 284 (35600), 245 (25400), 231 (28200) nm.

Synthesis of ***L*^{2}**

Prepared as for **L^{1}** but using 3–aminopropanol (0.31 mL, 3.98 mmol) and 2–(3'–nitro–4'–chlorophenyl)–1–phenyl–1H–imidazo[4,5-*f*][1,10]–phenanthroline (360 mg, 0.80 mmol) to give **L^{2}** as a red solid (yield = 349 mg, 89 %). ^{1}H NMR (400 MHz, $CDCl_3$): δ_H = 9.13 (d, 1H, $^{3}J_{HH}$ = 1.6 Hz), 9.05 (dd, 1H, J_{HH} = 8.1, 8.0 Hz), 9.00–8.97 (m, 1H), 8.18 (broad t, 1H, $^{3}J_{HH}$ = 4.6 Hz, N*H*), 8.15 (d, 1H, $^{3}J_{HH}$ = 2.2 Hz), 7.72–7.65 (m, 5H), 7.62–7.58 (m, 2H), 7.37 (dd, 1H, J_{HH} = 8.5, 8.4 Hz), 7.27 (dd, 1H, J_{HH} = 4.3, 2.3 Hz), 6.58 (d, 1H, $^{3}J_{HH}$ = 9.2 Hz), 3.83 (t, 2H, $^{3}J_{HH}$ = 5.7 Hz, HOCH_2), 3.34 (app. quar., 2H, $^{3}J_{HH}$ = 5.9 Hz, NHCH_2), 2.22 (broad s, 1H, O*H*), 1.91 (app. quin., 2H, $^{3}J_{HH}$ = 6.4 Hz, $NHCH_2CH_2$) ppm. HRMS (ES^+) found *m/z* 491.1821, calculated at 491.1826 for $[C_{28}H_{23}N_6O_3]^+$. IR (solid) ν_{max}: 3375, 2929, 2902, 2866, 1627, 1566, 1543, 1517, 1498, 1462, 1444, 1425, 1413, 1390, 1367, 1342, 1298, 1255, 1234, 1209, 1166, 1002, 912, 891, 866, 804, 83, 740, 704, 717, 671, 524, 408 cm^{-1}. UV-Vis (MeCN) λ_{max} ($\varepsilon/M^{-1}cm^{-1}$): 560 (3900), 446 (4800), 322 (10500), 282 (13400), 241 (11100), 228 (12100) nm.

Synthesis of ***L*^{3}**

L^{1} (207 mg, 0.40 mmol) and a 10 % loaded Pd/C catalyst (42 mg, 40 μmol) were stirred in methanol (15 mL) with H_2 gas delivered into the solvent, for 16 hrs, forming a green solution. The solution was filtered through Celite to remove the Pd/C and the methanol removed under vacuum to give **L^{3}** as a green crystalline solid (yield = 130 mg, 67 %). ^{1}H NMR (250 MHz, $CDCl_3$): δ_H = 9.17–9.03 (m, 2H), 9.01–8.90 (m, 1H), 7.72–7.51(m, 5H), 7.51–7.42 (m, 2H), 7.40–7.27 (m, 2H), 7.27–7.13 (m, 2H), 7.09 (s, 1H), 6.74 (dd, 1H, J_{HH} = 8.3, 8.2 Hz), 6.38 (d, 1H, $^{3}J_{HH}$ = 8.3 Hz), 3.66 (app. quin.,

4H, $NH_2CH_2CH_2$), 3.64 (t, 2H, $^3J_{HH}$ = 5.6 Hz, OCH_2CH_2), 3.21 (app. quar., 2H, $^3J_{HH}$ = 5.1 Hz, OCH_2CH_2) ppm. $^{13}C\{^1H\}$ NMR (75 MHz, $CDCl_3$): δ_C = 148.9, 139.2, 138.5, 133.6, 130.8, 130.5, 130.2, 129.2, 129.0, 128.0, 123.5, 122.3, 122.2, 119.9, 117.9, 110.7, 72.2, 69.2, 65.8, 61.8,43.6, 29.8, 27.4, 15.4 ppm. LRMS (AP^+) found *m/z* 491.22 for $[M+H]^+$; HRMS (ES^+) found *m/z* 491.2182, calculated at 491.2190 for $[C_{29}H_{27}N_6O_2]^+$. IR (solid) ν_{max}: 3334, 3234, 3062, 2926, 2864, 1598, 1562, 1543, 1494, 1469, 1446, 1392, 1377, 1338, 1327, 1296, 1276, 1238, 1163, 1118, 1064, 1033, 995, 927, 879, 802, 738, 707, 675, 621, 405 cm^{-1}. UV-Vis (MeCN) λ_{max} ($\varepsilon/M^{-1}cm^{-1}$): 333 (16600), 284 (26900), 255 (30172), 232 (31400) nm.

Synthesis of ***L*^{4}**

Prepared as for $\mathbf{L^3}$ but using $\mathbf{L^2}$ (272 mg, 0.56 mmol) and a 10% loaded Pd/C catalyst (59 mg, 56 μmol) to give $\mathbf{L^4}$ as a green crystalline solid (yield = 208 mg, 81 %). ^1H NMR (400 MHz, $CDCl_3$): δ_H 9.11–9.03 (m, 2H), 8.97–8.92 (m, 1H), 7.69–7.65 (m, 1H), 7.62–7.54 (m, 3H), 7.47 (d, 2H, $^3J_{HH}$ = 6.6 Hz), 7.33 (dd, 1H, J_{HH} = 8.4 , 8.1 Hz), 7.22–7.16 (m, 1H), 7.23 (s, 1H), 6.74 (dd, 1H, J_{HH} = 8.4, 8.3 Hz), 6.35 (d, 1H, $^3J_{HH}$ = 6.44 Hz), 3.74 (t, 2H, $^3J_{HH}$ = 5.7 Hz, $HOCH_2$), 3.14 (t, 2H, $^3J_{HH}$ = 5.7 Hz, $NHCH_2$), 1.91 (app quin, 2H, $^3J_{HH}$ = 6.0 Hz, $NHCH_2CH_2$) ppm. $^{13}C\{^1H\}$ NMR (151 MHz, $CDCl_3$): δ_C = 153.0, 148.8, 147.6, 144.6, 144.2, 139.5, 138.5, 135.9, 133.3, 130.6, 130.4, 130.1, 129.0, 127.9, 126.6, 123.9, 123.4, 122.3, 122.1, 119.9, 119.1, 117.7, 111.3, 61.6, 41.9, 31.7 ppm. HRMS (ES^+) found *m/z* 461.2080, calculated at 461.2084 for $[C_{28}H_{25}N_6O]^+$. IR (solid) ν_{max} = 3242, 3051, 2947, 1637, 1593, 1564, 1537, 1514, 1494, 1485, 1467, 1442, 1421, 1350, 1294, 1267, 1157, 1047, 908, 812, 779, 740, 721, 711, 640, 621, 507, 405 cm^{-1}. UV-Vis (MeCN): λ_{max} ($\varepsilon/M^{-1}cm^{-1}$) = 334 (29300), 281 (40000), 252 (48700), 231 (51600) nm.

Synthesis of ***L*^{5}**

NO(g) was slowly bubbled through a deaerated $CHCl_3$ solution of $\mathbf{L^3}$ (21 mg, 43.8 μmol) for 30 seconds in a sealed vessel during which time a rapid color change occurred. NO(g) delivery was ceased and the solution stirred for 5 minutes. The vessel was then opened to air and stirred for a further 30 minutes. The solvent was removed *in vacuo* and the sticky residue dissolved in minimal acetonitrile. Precipitation of the product was induced with the slow addition of diethyl ether and subsequent filtration and drying gave $\mathbf{L^5}$ as a yellow–orange solid (yield = 16 mg, 73 %). ^{1}H NMR (400 MHz, CD_3CN): δ_H = 9.72 (d, 1H, $^3J_{HH}$ = 7.0 Hz), 9.27 (dd, 1H, $^3J_{HH}$ = 5.2 Hz, $^3J_{HH}$ = 5.1 Hz), 9.14 (app. t, 1H), 8.41–8.36 (m, 1H), 8.14 (s, 1H), 8.01 (dd, 1H, J_{HH} = 8.8, 8.7 Hz), 7.95 (d, 1H, $^3J_{HH}$ = 9.1 Hz), 7.90–7.75 (m, 7H), 4.02 (t, 2H, $^3J_{HH}$ = 5.1 Hz, NCH_2), 3.66–3.31 (m, 4H, 2 × CH_2), 1.20 (t, 2H, $^3J_{HH}$ = 7.0 Hz, CH_2) ppm. LRMS (ES$^+$) found *m/z* 524.2 for $[M+Na]^+$; HRMS (ES$^+$) found *m/z* 502.1973, calculated at 502.1986 for $[C_{29}H_{24}N_7O_2]^+$. IR (solid) ν_{max}: 3344, 3062, 2924, 2873, 1612, 1577, 1543, 1496, 1477, 1442, 1338, 1315, 1242, 1172, 1126, 1060, 1041, 979, 864, 829, 806, 717, 621, 474, 412 cm^{-1}. UV-Vis (MeCN) λ_{max} (ε/M^{-1}cm^{-1}): 393 (1100), 300 (23300), 260 (29600), 228 (24000) nm.

Synthesis of ***L*^{6}**

Prepared as for $\mathbf{L^5}$ but using $\mathbf{L^4}$ (28 mg, 60.8 μmol) to give $\mathbf{L^6}$ as a yellow–orange solid (yield = 27 mg, 95 %). ^{1}H NMR (400 MHz, DMSO–*d6*): δ_H = 9.65 (d, 1H, $^3J_{HH}$ = 8.1 Hz), 9.31 (d, 1H, $^3J_{HH}$ = 4.9 Hz,), 9.18 (d, 1H, $^3J_{HH}$ = 4.2 Hz), 8.43–8.35 (m, 1H), 8.05 (s, 1H), 8.00–7.75 (m, 8H), 7.64 (d, 1H, $^3J_{HH}$ = 8.6 Hz), 4.76 (t, 2H, $^3J_{HH}$ = 6.8 Hz, NCH_2), 2.05 (app. quin., 2H, NCH_2CH_2) ppm (N.B. one CH_2 resonance was

obscured by the residual solvent peak from DMSO). $^{13}C\{^{1}H\}$ NMR (151 MHz, DMSO–*d6*): δ_C = 153.4, 147.2, 145.1, 137.1, 135.0, 133.8, 131.7, 131.5, 131.3, 129.3, 129.0, 128.0, 126.7, 126.1, 125.2, 125.1, 121.2, 120.6, 111.6, 71.5, 65.4, 58.0, 45.4, 45.0, 32.8, 31.2, 15.6 ppm. LRMS (ES^+) found *m/z* 472.3 for $[M+H]^+$ and 494.3 for $[M+Na]^+$; HRMS (ES^+) found *m/z* 472.1881, calculated at 472.1880 for $[C_{28}H_{22}N_7O]^+$. IR (solid) ν_{max}: 3394, 3074, 1603, 1577, 1543, 1496, 1473, 1438, 1384, 1315, 1280, 1242, 1165, 1126, 1072, 1037, 979, 945, 875, 829, 783, 717, 621, 540, 416 cm^{-1}. UV-Vis (MeCN) λ_{max} ($\varepsilon/M^{-1}cm^{-1}$): 412 (500), 299 (7400), 261 (11100), 230 (8800) nm.

General procedure for the synthesis of Ir(III) precursors

$[(C^N)_2Ir(\mu–Cl)_2Ir(C^N)_2]$ where (C^N = ppy or emptz) were synthesized according to the Nonoyama route[43][43] and used without further purification. $IrCl_3 \cdot xH_2O$ (0.200 g, 0.68 mmol) and the appropriate ligand (2.5 eq.) in 2–methoxyethanol (6 mL) and distilled water (2 mL) were heated at 120 °C for 48 h. The mixture was allowed to cool, and the product precipitated by addition of distilled water (30 mL). The yellow $[(ppy)_2Ir(\mu–Cl)_2Ir(ppy)_2]$ or red $[(emptz)_2Ir(\mu–Cl)_2Ir(emptz)_2]$ solids were collected by filtration, washed with distilled water, and dried in an oven. $[Ir(C^N)_2(MeCN)_2]BF_4$ and $[Ir(C^N)_2(\mathbf{L})]BF_4$ where (C^N = ppy and emptz) were synthesized following methods previously reported.[23]

Synthesis of $[Ir(ppy)_2(MeCN)_2]BF_4$

In a foil-wrapped flask, $AgBF_4$ (71 mg, 0.36 mmol) in MeCN (15 mL) was added to a stirred solution of $[(ppy)_2Ir(\mu–Cl)_2Ir(ppy)_2]$ (195 mg, 0.18 mmol) in hot MeCN (20 mL), under a dinitrogen atmosphere. The solution was then heated at reflux for 2 hours and cooled. Precipitation of the product was assisted by the addition of diethyl

ether and was subsequently filtered and dried to give $[Ir(ppy)_2(MeCN)_2]BF_4$ as a yellow powder (yield = 231 mg, 91 %). ^{1}H NMR (400 MHz, $CDCl_3$): δ_H = 9.02 (d, 2H, $^3J_{HH}$ = 5.8 Hz), 7.87–7.83 (m, 4H), 7.48 (d, 2H, $^3J_{HH}$ = 6.9 Hz), 7.35 (app t, 2H, $^3J_{HH}$ = 6.2 Hz), 6.84 (app t, 2H, $^3J_{HH}$ = 6.5 Hz), 6.69 (app t, 2H, $^3J_{HH}$ = 6.9 Hz), 6.02 (d, 2H, $^3J_{HH}$ = 7.6 Hz), 2.30 (s, 6H, C*H*$_3$CN) ppm.

Synthesis of $[Ir(emptz)_2(MeCN)_2]BF_4$

Prepared as for $[Ir(ppy)_2(MeCN)_2]BF_4$ but using $AgBF_4$ (71 mg, 0.36 mmol) and $[(emptz)_2Ir(\mu\text{–}Cl)_2Ir(emptz)_2]$ (149 mg, 0.11 mmol) to give $[Ir(emptz)_2(MeCN)_2]BF_4$ as a yellow powder (yield = 153 mg, 87 %). ^{1}H NMR (400 MHz, $CDCl_3$): δ_H = 7.53 (d, 2H, $^3J_{HH}$ = 6.7 Hz), 6.92 (dd, 4H, $^3J_{HH}$ = 7.5 Hz, $^3J_{HH}$ = 7.4 Hz), 6.84 (dd, 2H, $^3J_{HH}$ = 7.5, 6.8 Hz), 6.23 (d, 2H, $^3J_{HH}$ = 7.5 Hz), 4.46 (q, 4H, $^3J_{HH}$ = 7.1 Hz, CO_2CH_2), 3.04 (s, 6H, C*H*$_3$), 2.43 (s, 6H, C*H*$_3$CN), 1.47 (t, 6H, $^3J_{HH}$ = 6.4 Hz, $CO_2CH_2CH_3$) ppm.

Synthesis of $[Ir(ppy)_2(\mathbf{L^1})]BF_4$

L^1 (33.1 mg, 63.6 μmol) and $[Ir(ppy)_2(MeCN)_2]BF_4$ (42.6 mg, 63.6 μmol) were heated at reflux in $CHCl_3$ (10 mL) for 48 hours. The solvent was then reduced *in vacuo* and precipitation of the product induced by the slow addition of diethyl ether. Subsequent filtration and drying gave $[Ir(ppy)_2(\mathbf{L^1})]BF_4$ as an orange powder (yield = 57 mg, 80 %). ^{1}H NMR (400 MHz, $CDCl_3$): δ_H = 9.32 (d, 1H, $^3J_{HH}$ = 8.4 Hz), 8.45 (broad t, 1H, $^3J_{HH}$ = 3.6 Hz, N*H*), 8.41 (d, 1H, $^3J_{HH}$ = 2.4 Hz), 8.26 (d, 1H, $^3J_{HH}$ = 3.6 Hz), 8.15 (d, 1H, $^3J_{HH}$ = 4.8 Hz), 7.91–7.65 (m, 13H), 7.53–7.47 (m, 2H), 7.37 (d, 1H, $^3J_{HH}$ = 6.8 Hz), 7.10–7.02 (m, 3H), 6.96 (app. t, 2H), 6.89–6.84 (m, 2H), 6.39 (d, 2H, $^3J_{HH}$ = 7.6 Hz), 3.79 (app quar, 4H, 2 × C*H*$_2$), 3.68–3.62 (m, 2H, C*H*$_2$), 3.55–3.50 (m, 2H, C*H*$_2$), 0.81 (broad s, 1H, O*H*) ppm. ^{13}C{^{1}H} NMR (151 MHz, $CDCl_3$): δ_C = 168.1,

167.3, 152.7, 150.5, 149.9, 149.5, 149.1, 148.7, 148.4, 145.8, 145.0, 144.9, 143.9, 143.4, 138.1, 138.0, 136.8, 136.7, 136.4, 132.9, 132.1, 131.8, 131.7, 131.6, 131.4, 131.0, 130.7, 130.6, 129.1, 128.6, 128.1, 128.0, 127.9, 126.6, 126.4, 126.2, 124.8, 124.7, 123.9, 123.1, 122.8, 12.7, 119.6, 119.4, 116.4, 114.3, 114.1 ppm. LRMS (ES^+) found *m/z* 1019.3 for $[M]^+$; HRMS (ES^+) found *m/z* 1019.2761, calculated at 1019.2772 for $[C_{51}H_{40}N_8O_4Ir]^+$. IR (solid) ν_{max}: 3533, 3369, 3045, 2937, 2872, 1627, 1606, 1579, 1519, 1477, 1448, 1381, 1352, 1305, 1276, 1238, 1161, 1118, 1053, 1031, 829, 630, 759, 729, 669, 630, 540, 518, 415 cm^{-1}. UV-Vis (MeCN) λ_{max} ($\varepsilon/M^{-1}cm^{-1}$): 455 (5900) sh, 412 (10300) sh, 318 (44500) sh, 290 (59000) sh, 269 (68100) nm.

Synthesis of $[Ir(ppy)_2(\mathbf{L^2})]BF_4$

Prepared as for $[Ir(ppy)_2(\mathbf{L^1})_2]BF_4$ but using $\mathbf{L^2}$ (36.5 mg, 74.4 μmol) and $[Ir(ppy)_2(MeCN)_2]BF_4$ (49.8 mg, 74.4 μmol) to give $[Ir(ppy)_2(\mathbf{L^2})]BF_4$ as a yellow powder (yield = 61.7 mg, 57 %). ^1H NMR (400 MHz, $CDCl_3$): δ_H = 9.33 (d, 1H, $^3J_{HH}$ = 7.6 Hz), 8.14–8.10 (m, 1H), 7.91–7.12 (m, 13H), 7.52–7.44 (m, 3H), 7.35 (d, 1H, $^3J_{HH}$ = 6.7 Hz), 7.06–6.78 (m, 7H), 6.37 (d, 2H, $^3J_{HH}$ = 8.3 Hz), 3.77 (t, 2H, $^3J_{HH}$ = 5.7 Hz, NHCH_2), 2.11 (t, 2H, $^3J_{HH}$ = 4.2 Hz, CH_2OH), 1.96–1.88 (m, 2H, $NHCH_2CH_2$), 0.81 (broad s, 1H, O*H*) ppm. $^{13}C\{^1H\}$ NMR (151 MHz, $CDCl_3$): δ_C = 167.3, 152.8, 149.3, 148.4, 145.7, 143.8, 143.2, 138.1, 138.0, 136.7, 136.4, 132.1, 131.8, 131.7, 131.3, 131.2, 131.0, 129.1, 127.9, 126.4, 126.2, 124.8, 124.7, 123.9, 123.1, 122.7, 119.6, 119.4, 116.0, 114.3, 60.3, 40.5, 31.3, 29.7 ppm. LRMS (ES^+) found *m/z* 989.3 for $[M]^+$; HRMS (ES^+) found *m/z* 989.2673, calculated at 989.2673 for $[C_{50}H_{38}N_8O_3Ir]^+$. IR (solid) ν_{max}: 3547, 3365, 3059, 2929, 2875, 1627, 1606, 1577,

1527, 1496, 1477, 1448, 1419, 1303, 1267, 1230, 1157, 1055, 1031, 894, 808, 758, 711, 669, 630, 518. 417 cm^{-1}. UV-Vis (MeCN) λ_{max} ($\varepsilon/M^{-1}cm^{-1}$): 456 (5300) sh, 414 (7800) sh, 316 (37300) sh, 293 (46400) sh, 269 (54900) nm.

*Synthesis of [Ir(ppy)$_2$(**L^3**)]BF$_4$*

Prepared as for [Ir(ppy)$_2$(**L^1**)]BF$_4$ but using **L^3** (29.4 mg, 59.9 μmol) and [Ir(ppy)$_2$(MeCN)$_2$]BF$_4$ (40.1 mg, 59.9 μmol) to give [Ir(ppy)$_2$(**L^3**)]BF$_4$ as a pale green powder (yield = 53 mg, 82 %). ^{1}H NMR (400 MHz, $CDCl_3$): δ_H = 9.35 (d, 1H, $^3J_{HH}$ = 8.1 Hz), 8.45 (broad t, 1H, $^3J_{HH}$ = 3.6 Hz, N*H*), 8.41 (s, 1H), 8.25 (d, 1H, $^3J_{HH}$ = 4.3 Hz), 8.14 (d, 1H, $^3J_{HH}$ = 4.1 Hz), 7.92–7.65 (m, 13H), 7.53–7.47 (m, 3H), 7.37 (d, 1H, $^3J_{HH}$ = 5.1 Hz), 7.11–6.81 (m, 7H), 6.40 (d, 2H, $^3J_{HH}$ = 7.5 Hz), 3.76–3.69 (m, 4H, 2 × C*H*$_2$), 3.60 (t, 2H, $^3J_{HH}$ = 4.7 Hz, C*H*$_2$), 3.47 (t, 2H, $^3J_{HH}$ = 4.6 Hz, C*H*$_2$), 0.82 (broad s, 1H, O*H*) ppm. ^{13}C{^{1}H} NMR (151 MHz, CD_3CN): δ_C = 167.5, 155.6, 150.6, 150.3, 149.5, 149.3, 148.4, 144.8, 144.7, 144.2, 139.1, 138.5, 137.7, 136.8, 134.4, 132.4, 131.7, 130.9, 130.8, 130.7, 130.4, 129.9, 128.8, 128.7, 127.8, 127.0, 126.4, 125.9, 124.9, 123.4, 123.3, 122.6, 122.6, 121.2, 119.8, 119.8, 117.3, 109.5, 72.368.9, 61.0, 43.2, ppm. LRMS (ES$^+$) found *m/z* 989.3 for [M]$^+$; HRMS (ES$^+$) found *m/z* 989.3051, calculated at 989.3037 for $[C_{51}H_{42}N_8O_2Ir]^+$. IR (solid) ν_{max}: 3369, 3062, 2960, 2924, 2363, 1606, 1581, 1477, 1419, 1381, 1352, 1338, 1303, 1261, 1226, 1161, 1030, 950, 883, 806, 758, 727, 669, 518, 415 cm^{-1}. UV-Vis (MeCN) λ_{max} ($\varepsilon/M^{-1}cm^{-1}$): 433 (9000) sh, 403 (12100), 315 (47600) sh, 292 (61400), 268 (63000) nm.

*Synthesis of [Ir(ppy)$_2$(**L^4**)]BF$_4$*

Prepared as for [Ir(ppy)$_2$(**L^1**)]BF$_4$ but using **L^4** (35.0 mg, 76.5 μmol) and [Ir(ppy)$_2$(MeCN)$_2$]BF$_4$ (51.2 mg, 76.5 μmol) to give [Ir(ppy)$_2$(**L^4**)]BF$_4$ as a brown

powder (yield = 62 mg, 77 %). ^{1}H NMR (400 MHz, $CDCl_3$): δ_H = 9.32 (d, 1H, $^{3}J_{HH}$ = 7.6 Hz), 8.23 (d, 1H, $^{3}J_{HH}$ = 5.0 Hz), 8.11 (d, 1H, $^{3}J_{HH}$ = 4.0 Hz), 7.90 (d, 2H, $^{3}J_{HH}$ = 8.1 Hz), 7.84–7.79 (m, 1H), 7.77–7.56 (m, 10H), 7.48–7.42 (m, 3H), 7.34 (d, 1H, $^{3}J_{HH}$ = 5.2 Hz), 7.10–6.84 (m, 6H), 6.38 (d, 2H, $^{3}J_{HH}$ = 7.7 Hz), 3.72 (t, 2H, $^{3}J_{HH}$ = 5.8 Hz, NHC*H*$_2$), 3.22 (t, 2H, $^{3}J_{HH}$ = 6.4 Hz, C*H*$_2$OH), 1.82–1.80 (m, 2H, NHCH$_2$C*H*$_2$), 0.84 (broad s, 1H, O*H*) ppm. ^{13}C{^{1}H} NMR (151 MHz, CD_3CN): δ_C = 167.5, 156.1, 150.5, 150.2, 149.4, 149.3, 148.4, 144.8, 144.2, 139.3, 138.4, 134.2, 132.4, 131.7, 131.6, 131.4, 130.9, 130.4, 128.9, 128.8, 128.7, 126.9, 126.5, 125.9, 124.9, 123.4, 122.6, 121.2, 119.8, 115.9, 109.0, 59.7, 40.7, 31.7 ppm. LRMS (AP$^+$) found *m/z* 959.3 for [M]$^+$; HRMS (ES$^+$) found *m/z* 959.2928, calculated at 959.2931 for $[C_{50}H_{40}N_8OIr]^+$. IR (solid) ν_{max}: 3354, 3041, 2937, 2875, 1606, 1581, 1477, 1419, 1381, 1303, 1269, 1157, 1051, 1030, 808, 758, 727, 669, 630, 524, 403 cm^{-1}. UV-Vis (MeCN) λ_{max} (ε/M^{-1}cm^{-1}): 466 (2900), 410 (11800), 344 (24900), 288 (49000), 264 (69600) nm.

*Synthesis of [Ir(emptz)$_2$(**L^4**)]BF$_4$*

Prepared as for [Ir(ppy)$_2$(**L^1**)]BF$_4$ but using **L^4** (36.2 mg, 78.6 μmol) and [Ir(emptz)$_2$(MeCN)$_2$]BF$_4$ (67.1 mg, 78.6 μmol) to give [Ir(emptz)$_2$(**L^4**)]BF$_4$ as an orange powder (yield = 86 mg, 89 %). ^{1}H NMR (400 MHz, $CDCl_3$): δ_H = 9.40 (d, 1H, $^{3}J_{HH}$ = 8.3 Hz), 8.19 (d, 1H, $^{3}J_{HH}$ = 4.9 Hz), 8.07 (d, 1H, $^{3}J_{HH}$ = 4.9 Hz), 7.97–7.90 (m, 1H), 7.80–7.51 (m, 9H), 7.14 (app quar, 2H), 7.08 (app quar, 2H), 6.92 (d, 1H, $^{3}J_{HH}$ = 9.9 Hz), 6.52 (app t, 2H), 6.43 (d, 1H, $^{3}J_{HH}$ = 8.6 Hz), 4.29–4.21 (m, 4H, 2 × CO$_2$C*H*$_2$), 3.70 (t, 2H, $^{3}J_{HH}$ = 5.5 Hz, NHC*H*$_2$), 3.15 (t, 2H, C*H*$_2$OH), 1.79 (app t, 2H, NHCH$_2$C*H*$_2$), 1.58 (s, 6H, C*H*$_3$), 1.29 (t, 6H, $^{3}J_{HH}$ = 7.1 Hz, CO$_2$CH$_2$C*H*$_3$) ppm. ^{13}C{^{1}H} NMR (151 MHz, $CDCl_3$): δ_C = 182.5, 160.3, 160.2, 158.5, 158.4, 156.2, 149.2, 149.1, 140.0, 144.7, 140.1, 140.0, 139.9, 136.9, 136.7, 133.4, 133.2, 132.5,

132.4, 131.3, 131.2, 130.8, 128.5, 128.5, 126.6, 126.4, 126.2, 123.8, 123.7, 120.2, 120.0, 62.3, 62.2, 61.2, 53.4, 41.7, 31.3, 14.6, 14.5, 14.1 ppm. LRMS (AP^+) found *m/z* 1143.3 for $[M]^+$; HRMS (ES^+) found *m/z* 1143.2815, calculated at 1143.2795 for $[C_{54}H_{48}N_8O_5S_2Ir]^+$. IR (solid) ν_{max}: 3379, 3061, 2931, 1710, 1598, 1583, 1552, 1496, 1440, 1373, 1327, 1288, 1257, 1159, 1128, 1097, 1055, 1004, 810, 761, 671, 543, 428 cm^{-1}. UV-Vis (MeCN) λ_{max} ($\varepsilon/M^{-1}cm^{-1}$): 418 (13600), 355 (31800), 316 (50700), 294 (61100), 263 (56800) nm.

Synthesis of $[Ir(ppy)_2(\mathbf{L^5})]BF_4$

Prepared as for $\mathbf{L^5}$ but using $[Ir(ppy)_2(\mathbf{L^3})]BF_4$ (25.1 mg, 23.2 μmol) to give $[Ir(ppy)_2(\mathbf{L^5})]BF_4$ as a brown solid (yield = 24.2 mg, 96 %). ^{1}H NMR (400 MHz, CD_3CN): δ_H = 9.29 (d, 1H, $^3J_{HH}$ = 7.6 Hz), 8.33 (d, 1H, $^3J_{HH}$ = 5.6 Hz), 8.19 (d, 1H, $^3J_{HH}$ = 4.8 Hz), 8.10–7.64 (m, 16H), 7.53–7.47 (m, 3H), 7.13–7.07 (m, 2H), 7.01–6.87 (m, 4H), 6.93 (app t, 2H), 4.84 (t, 2H, $^3J_{HH}$ = 4.8 Hz, NCH_2), 3.96 (t, 2H, $^3J_{HH}$ = 4.8 Hz, CH_2), 3.47–3.42 (m, 4H, 2 × CH_2) ppm. HRMS (ES^+) found *m/z* 1000.2834, calculated at 1000.2827 for $[C_{51}H_{39}N_9O_2Ir]^+$. IR (solid) ν_{max}: 3395, 3064, 1606, 1583, 1496, 1477, 1438, 1417, 1305, 1226, 1053, 1031, 885, 810, 759, 727, 669, 630, 460, 416, 408 cm^{-1}. UV-Vis (MeCN) λ_{max} ($\varepsilon/M^{-1}cm^{-1}$): 463 (2000) sh, 382 (9300), 341 (16700), 293 (46200), 267 (68500) nm.

Synthesis of $[Ir(ppy)_2(\mathbf{L^6})]BF_4$

Prepared as for $\mathbf{L^5}$ but using $[Ir(ppy)_2(\mathbf{L^4})]BF_4$ (21.5 mg, 20.5 μmol) to give $[Ir(ppy)_2(\mathbf{L^6})]BF_4$ as a yellow–brown solid (yield = 17.5 mg, 81 %). ^{1}H NMR (400 MHz, CD_3CN): δ_H = 9.33 (d, 2H, $^3J_{HH}$ = 8.0 Hz), 8.71 (dd, 2H, J_{HH} = 13.0, 12.9 Hz), 8.34 (app t, 2H), 8.27 (d, 1H, $^3J_{HH}$ = 5.3 Hz), 8.06–7.92 (m, 10H), 7.84–7.67 (m, 4H),

7.09–7.03 (m, 2H), 6.66 (dd, 1H, $^3J_{HH}$ = 8.5, 8.4 Hz), 4.76 (t, 2H, $^3J_{HH}$ = 7.3 Hz, NHCH_2), 3.51 (t, 2H, $^3J_{HH}$ = 6.0 Hz, CH_2OH), 2.46–2.37 (m, 2H, NCH$_2$CH_2) ppm. LRMS (ES$^+$) found *m/z* 973.4 for [M]$^+$; HRMS (ES$^+$) found *m/z* 973.1699, calculated at 973.2828 for [$C_{50}H_{38}N_9OIr$]$^+$. IR (solid) ν_{max}: 3456, 3114, 1612, 1589, 1573, 1504, 1481, 1454, 1334, 1284, 1226, 1165, 1107, 1056, 1034, 883, 783, 756, 740, 725, 648, 420 cm^{-1}. UV-Vis (MeCN) λ_{max} (ε/M^{-1}cm^{-1}): 392 (9100), 342 (15500) sh, 287 (35800) sh, 263 (44200) nm.

*Synthesis of [Ir(emptz)$_2$(**L**^{6})]BF$_4$*

Prepared as for **L**^{5} but using [Ir(emptz)$_2$(**L**^{4})]BF$_4$ (34.5 mg, 28.0 μmol) to give [Ir(emptz)$_2$(**L**^{6})]BF$_4$ as a yellow solid (yield = 29.4 mg, 84 %). ^{1}H NMR (400 MHz, $CDCl_3$): δ_H = 9.48–9.39 (m, 1H), 8.59 (d, 1H, $^3J_{HH}$ = 11.0 Hz), 8.27–7.52 (m, 15H), 7.23–7.10 (m, 2H), 7.10–6.99 (m, 2H), 6.52 (app t, 1H), 4.82–4.79 (m, 2H, NHCH_2), 4.33–4.19 (m, 4H, CO$_2$CH_2), 3.60 (t, 2H, $^3J_{HH}$ = 5.2 Hz, CH_2OH), 2.26–2.16 (m, 2H, NCH$_2$CH_2), 1.60 (s, 6H, CH_3), 1.29 (t, 6H, $^3J_{HH}$ = 6.8 Hz, CO$_2$CH$_2$CH_3) ppm. LRMS (ES$^+$) found *m/z* 1154.3 for [M]$^+$; HRMS (ES$^+$) found *m/z* 1154.2594, calculated at 1154.2585 for [$C_{54}H_{45}N_9O_5S_2Ir$]$^+$. IR (solid) ν_{max}: 3400, 3059, 2980, 1714, 1697, 1618, 1583, 1554, 1498, 1440, 1388, 1327, 1288, 1253, 1163, 1129, 1004, 875, 812, 761, 727, 547, 415 cm^{-1}. UV-Vis (MeCN) λ_{max} (ε/M^{-1}cm^{-1}): 403 (12000) sh, 355 (19300) sh, 313 (49200) sh, 293 (61400), 268 (63000) nm.

Acknowledgements

We thank Cardiff University for financial support and the staff of the EPSRC Mass Spectrometry National Service (University of Swansea) for providing MS data.

Access to the Cardiff University Advanced Research Computing facility “ARCCA” is gratefully acknowledged.

Supplementary Information

Examples of NMR and MS characterization data, Cartesian coordinates of all calculated structures in a format for convenient visualizationand details of all excited states are provided in the SI.

References

[1] a) M.A. Baldo, M.E. Thompson, S.R. Forrest, Nature 403 (2000) 750; b) A.B. Tamayo, B.D. Alleyne, P.I. Djurovich, S. Lamansky, I. Tsyba, N.N. Ho, R. Bau, M.E. Thompson, J. Am. Chem. Soc. 125 (2003) 7377; c) S. Lamansky, P. Djurovich, D. Murphy, F. Abdel-Razzaq, R. Kwong, I. Tsyba, M. Bortz, B. Mui, R. Bau, M.E. Thompson, Inorg. Chem. 40 (2001) 1704; d) A.F. Henwood, E. Zysman-Colman, Chem. Commun. 53 (2017) 807.

[2] E. Baranoff, J-H. Yum, M. Grätzel and Md. K. Nazeeruddin, J. Organomet. Chem. 694 (2009) 2661

[3] a) I-S. Shin, H-C. Lim, J-W. Oh, J-K. Lee, T. H. Kim and H. Kim, Electrochem. Commun. 13 (2011) 64; b) H-C. Su, Y-H. Lin, C-H. Chang, H-W. Lin, C-C. Wu, F-C. Fang, H-F. Chen and K-T. Wong, J. Mater. Chem. 20 (2010) 5521; c) L. He, L. Duan, J. Qiao, G. Dong, L. Wang and Y. Qiu, Chem. Mater. 22 (2010) 3535; d) C. Rothe, C-J. Chiang, V. Jankus, K. Abdullah, X. Zeng, R. Jitchati, A. S. Batsanov, M. R. Bryce and A. P. Monkman, Adv. Funct. Mater. 19 (2009) 2038; e) S. Graber, K. Doyle, M. Neuburger, C. E. Housecroft, E. C. Constable, R. D. Costa, E. Orti, D. Repetto and H. J. Bolink, J. Am. Chem. Soc. 130 (2008) 14944

[4] For example: a) J.I. Goldsmith, W.R. Hudson, M.S. Lowry, T.H. Anderson, S. Bernhard, J. Am. Chem. Soc. 127 (2005) 7502; b) S-Y. Takizawa, R. Aboshi, S. Murata, Photochem. Photobiol. Sci. 10 (2011) 895; c) A. J. Hallett, N. White, W. Wu, X. Cui, P. N. Horton, S. J. Coles, J. Zhao, S. J. A. Pope, Chem. Commun. 48 (2012) 10838

[5] E. Baranoff, J-H. Yum, I. Jung, R. Vulcano, M. Grätzel and Md. K. Nazeeruddin, Chem. Asian J. 5 (2010) 496

[6] V. Fernández-Moreira, F. L. Thorp-Greenwood and M. P. Coogan, Chem. Commun. 46 (2010) 186

[7] G-G. Shan, H-B. Li, H-T. Cao, D-X. Zhu, P. Li, Z-M. Su, Y. Liao, Chem. Commun. 48 (2012) 2000.

[8] H. Sun, S. Liu, W. Lin, K.Y. Zhang, W. Lv, X. Huang, F. Huo, H. Yang, G. Jenkins, Q. Zhao, W. Huang, Nat. Commun. 5 (2014) 3601

[9] R.O. Bonello, M.B. Pitak, S.J. Coles, A.J. Hallett, I.A. Fallis, S.J.A. Pope, J. Organomet. Chem. 841 (2017) 39

[10] M. Finsgar, I. Milosev, Corrosion Sci. 52 (2010) 2737

[11] I. Briguglio, S. Piras, P. Corona, E. Gavini, M. Nieddu, G. Boatto, A. Carta, Eur. J. Med. Chem. 97 (2015) 612

[12] For example: F.A. Brede, F. Muhlbach, G. Sexti, K. Muller-Buschbaum, Dalton Trans. 45 (2016) 10609

[13] For example: a) X-J. Quan, Z-H. Ren, Y-Y. Wang, Z-H. Guan, Org. Lett. 16 (2014) 5728; b) J. Barluenga, C. Valdes, G. Beltran, M. Escribano, F. Aznar, Angew. Chem. Int. Ed. 45 (2006) 6893; c) A. Kolarovic, M. Schnurch, M.D. Mihovilovic, J. Org. Chem. 76 (2011) 2613; d) Y.M.A. Yamada, S.M. Sarkar, Y. Uozumi, J. Am. Chem. Soc. 134 (2012) 9285

[14] For example: Y. Jiang, Q. Kuang, Synlett (2009) 3163

[15] K.K-W. Lo, Acc. Chem. Res. 48 (2015) 2985

[16] A.W-T. Choi, C-S. Poon, H-W. Liu, H-K.Cheng, K.K-W. Lo, New J. Chem. 37 (2013) 1711

[17] W.H-T. Law, K-K. Leung, L.C-C. Lee, C-S. Poon, H-W. Liu, K.K-W. Lo, ChemMedChem. 9 (2014) 1316

[18] D. Tordera, A. Pertegas, N.M. Shavaleev, R. Scopelliti, E. Orti, H.J. Bolink, E. Baranoff, M. Gratzel, M.K. Nazeeruddin, J. Mat. Chem. 22 (2012) 19264

[19] N.N. Serveega, M. Donnier-Marechal, G. Vaz, A.M. Davies, M.O. Senge, J. Inorg. Biochem. 105 (2011) 1589

[20] Q. Sun, R. Wu, S. Cai, Y. Lin, L. Sellers, K. Sakamoto, B. He, B.R. Peterson, J. Med. Chem. 54 (2011) 1126

[21] For helpful reviews see: (a) S. Ladouceur, E. Zyzman-Colman, Eur. J. Inorg. Chem. (2013) 2985; (b) A.F. Henwood, E. Zysman-Colman, Chem. Commun. 53 (2016) 807

[22] Y-J. Yuan, Z-T. Yu, H-L. Gao, Z-G. Zou, C. Zheng, W. Huang, Chem. Eur. J. 19 (2013) 6340

[23] E.C. Stokes, E.E. Langdon-Jones, L.M. Groves, J.A. Platts, P.N. Horton, I.A. Fallis, S.J. Coles, S.J.A. Pope, Dalton Trans. 44 (2015) 8488

[24] J. Hu, M.R. Whittaker, H. Duong, Y. Li, C. Boyer, T.P. Davis, Angew. Chem. Int. Ed. 53 (2014) 7779

[25] (a) K.J. Castor, K.L. Metera, U.M. Tefashe, C.J. Serpell, J. Mauzeroll, H.F. Sleiman, Inorg. Chem. 54 (2015) 6958; (b) E.E. Langdon-Jones, A.J. Hallett, J.D. Routledge, D.A. Crole, B.D. Ward, J.A. Platts, S.J.A. Pope, Inorg. Chem. 52 (2013) 448

[26] J. Jayabharathi, R. Sathishkumar, V. Thanikachalam, K. Jayamoorthy, J. Fluoresc. 24 (2014) 445

[27] a) A.D. Becke, J. Chem. Phys. 98 (1993) 5648; b) C. T. Lee, W.T. Yang, R.G. Parr, Phys. Rev. B 37 (1988) 785

[28] Y. Zhao, D. G. Truhlar, Theor. Chem. Acc. 120 (2008) 215

[29] E. V. Ganin, A. E. Masunov, A. V. Siminel, M. S. Fonari, J. Phys. Chem. C 117 (2013) 18154

[30] P. J. Stephens, N. Harada, Chirality 22 (2010) 229

[31] J. Sun, W. Wu, H. Guo, J. Zhao, Eur. J. Inorg. Chem. (2011) 3165

[32] R.O. Bonello, I.R. Morgan, B.R. Yeo, L.E.J. Jones, B.M. Kariuki, I.A. Fallis, S.J.A. Pope, J. Organomet. Chem. 749 (2014) 150.

[33] C. Jin, J. Liu, Y. Chen, L. Zeng, R. Guan, C. Ouyang, L. Ji, H. Chao, Chem. Eur. J. 21 (2015) 12000

[34] S. Lamansky, P. Djurovich, D. Murphy, F. Abdel-Razzaq, H-E. Lee, C. Adachi, P.E. Burrows, S.R. Forrest, M.E. Thompson, J. Am. Chem. Soc. 123 (2001) 4304

[35] M. J. Frisch, G. W. Trucks, H. B. Schlegel, G. E. Scuseria, M. A. Robb, J.R. Cheeseman, G. Scalmani, V. Barone, B. Mennucci, G. A. Petersson, H. Nakatsuji, M. Caricato, X. Li, H. P. Hratchian, A. F. Izmaylov, J. Bloino, G. Zheng, J. L. Sonnenberg, M. Hada, M. Ehara, K. Toyota, R. Fukuda, J. Hasegawa, M. Ishida, T. Nakajima, Y. Honda, O. Kitao, H. Nakai, T. Vreven, J. A. Montgomery Jr, J. E. Peralta, F. Ogliaro, M. Bearpark, J. J. Heyd, E. Brothers, K. N. Kudin, V. N. Staroverov, T. Keith, R. Kobayashi, J. Normand, K. Raghavachari, A. Rendell, J. C. Burant, S. S. Iyengar, J. Tomasi, M. Cossi, N. Rega, J. M. Millam, M. Klene, J. E. Knox, J. B. Cross, V. Bakken, C. Adamo, J. Jaramillo, R. Gomperts, R. E. Stratmann, O. Yazyev, A. J. Austin, R. Cammi, C. Pomelli, J. W. Ochterski, R. L. Martin, K. Morokuma, V. G. Zakrzewski, G.

A. Voth, P. Salvador, J. J. Dannenberg, S. Dapprich, A. D. Daniels, O. Farkas, J. B. Foresman, J. V. Ortiz, J. Cioslowski, D. J. Fox, Gaussian 09, Revision C.01; Gaussian Inc.: Wallingford CT, 2010.

[36] T. Yanai, D. P. Tew, N. C. Handy, Chem. Phys. Lett. 393 (2004) 51

[37] S. Grimme, J. Antony, S. Ehrlich, H. Krieg, J. Chem. Phys. 132 (2010) 154104

[38] a) D. Andrae, U. Haussermann, M. Dolg, H. Stoll, H. Preuss, Theor. Chim. Acta 77 (1990) 123; b) T. H. Dunning Jr. J. Chem. Phys. 90 (1989) 1007.

[39] A. Vlček, S. Zalis, Coord. Chem. Rev. 251 (2007) 258

[40] J. Tomasi, B. Mennucci, R. Cammi, Chem. Rev. 105 (2005) 2999

[41] a) M. Frank, M. Nieger, F. Vogtle, P. Belser, A. von Zelewsky, L. de Cola, V. Balzani, F. Barigelletti, L. Flamigni, Inorg. Chim. Acta 242 (1996) 281; b) A. Juris, V. Balzani, F. Barigelletti, S. Campagna, P. Belser, A. von Zelewsky, Coord. Chem. Rev. 84 (1988) 85.

[42] N.M. Shavaleev, H. Adams, J.A. Weinstein, Inorg. Chim. Acta 360 (2007) 700

[43] M. Nonoyama, Bull. Chem. Soc. Jpn. 47 (1974) 767

References

[1] a) M.A. Baldo, M.E. Thompson, S.R. Forrest, Nature 403 (2000) 750; b) A.B. Tamayo, B.D. Alleyne, P.I. Djurovich, S. Lamansky, I. Tsyba, N.N. Ho, R. Bau, M.E. Thompson, J. Am. Chem. Soc. 125 (2003) 7377; c) S. Lamansky, P. Djurovich, D. Murphy, F. Abdel-Razzaq, R. Kwong, I. Tsyba, M. Bortz, B. Mui, R. Bau, M.E. Thompson, Inorg. Chem. 40 (2001) 1704; d) A.F. Henwood, E. Zysman-Colman, Chem. Commun. 53 (2017) 807.

[2] E. Baranoff, J-H. Yum, M. Grätzel and Md. K. Nazeeruddin, J. Organomet. Chem. 694 (2009) 2661.

[3] a) I-S. Shin, H-C. Lim, J-W. Oh, J-K. Lee, T. H. Kim and H. Kim, Electrochem. Commun. 13 (2011) 64; b) H-C. Su, Y-H. Lin, C-H. Chang, H-W. Lin, C-C. Wu, F-C. Fang, H-F. Chen and K-T. Wong, J. Mater. Chem. 20 (2010) 5521; c) L. He, L. Duan, J. Qiao, G. Dong, L. Wang and Y. Qiu, Chem. Mater. 22 (2010) 3535; d) C. Rothe, C-J. Chiang, V. Jankus, K. Abdullah, X. Zeng, R. Jitchati, A. S. Batsanov, M. R. Bryce and A. P. Monkman, Adv. Funct. Mater. 19 (2009) 2038; e) S. Graber, K. Doyle, M. Neuburger, C. E. Housecroft, E. C. Constable, R. D. Costa, E. Orti, D. Repetto and H. J. Bolink, J. Am. Chem. Soc. 130 (2008) 14944.

[4] For example: a) J.I. Goldsmith, W.R. Hudson, M.S. Lowry, T.H. Anderson, S. Bernhard, J. Am. Chem. Soc. 127 (2005) 7502; b) S-Y. Takizawa, R. Aboshi, S. Murata, Photochem. Photobiol. Sci. 10 (2011) 895; c) A. J. Hallett, N. White, W. Wu, X. Cui, P. N. Horton, S. J. Coles, J. Zhao, S. J. A. Pope, Chem. Commun. 48 (2012) 10838

[5] E. Baranoff, J-H. Yum, I. Jung, R. Vulcano, M. Grätzel and Md. K. Nazeeruddin, Chem. Asian J. 5 (2010) 496.

[6] V. Fernández-Moreira, F. L. Thorp-Greenwood and M. P. Coogan, Chem. Commun. 46 (2010) 186.

[7] G-G. Shan, H-B. Li, H-T. Cao, D-X. Zhu, P. Li, Z-M. Su, Y. Liao, Chem. Commun. 48 (2012) 2000.

[8] H. Sun, S. Liu, W. Lin, K.Y. Zhang, W. Lv, X. Huang, F. Huo, H. Yang, G. Jenkins, Q. Zhao, W. Huang, Nat. Commun. 5 (2014) 3601.

[9] R.O. Bonello, M.B. Pitak, S.J. Coles, A.J. Hallett, I.A. Fallis, S.J.A. Pope, J. Organomet. Chem. 841 (2017) 39.

[10] M. Finsgar, I. Milosev, Corrosion Sci. 52 (2010) 2737.

[11] I. Briguglio, S. Piras, P. Corona, E. Gavini, M. Nieddu, G. Boatto, A. Carta, Eur. J. Med. Chem. 97 (2015) 612.

[12] For example: F.A. Brede, F. Muhlbach, G. Sexti, K. Muller-Buschbaum, Dalton Trans. 45 (2016) 10609.

[13] For example: a) X-J. Quan, Z-H. Ren, Y-Y. Wang, Z-H. Guan, Org. Lett. 16 (2014) 5728; b) J. Barluenga, C. Valdes, G. Beltran, M. Escribano, F. Aznar, Angew. Chem. Int. Ed. 45 (2006) 6893; c) A. Kolarovic, M. Schnurch, M.D. Mihovilovic, J. Org. Chem. 76 (2011) 2613; d) Y.M.A. Yamada, S.M. Sarkar, Y. Uozumi, J. Am. Chem. Soc. 134 (2012) 9285.

[14] For example: Y. Jiang, Q. Kuang, Synlett (2009) 3163.

[15] K.K-W. Lo, Acc. Chem. Res. 48 (2015) 2985.

[16] A.W-T. Choi, C-S. Poon, H-W. Liu, H-K.Cheng, K.K-W. Lo, New J. Chem. 37 (2013) 1711

[17] W.H-T. Law, K-K. Leung, L.C-C. Lee, C-S. Poon, H-W. Liu, K.K-W. Lo, ChemMedChem. 9 (2014) 1316.

[18] D. Tordera, A. Pertegas, N.M. Shavaleev, R. Scopelliti, E. Orti, H.J. Bolink, E. Baranoff, M. Gratzel, M.K. Nazeeruddin, J. Mat. Chem. 22 (2012) 19264

[19] N.N. Serveega, M. Donnier-Marechal, G. Vaz, A.M. Davies, M.O. Senge, J. Inorg. Biochem. 105 (2011) 1589

[20] Q. Sun, R. Wu, S. Cai, Y. Lin, L. Sellers, K. Sakamoto, B. He, B.R. Peterson, J. Med. Chem. 54 (2011) 1126.

[21] For helpful reviews see: (a) S. Ladouceur, E. Zyzman-Colman, Eur. J. Inorg. Chem. (2013) 2985; (b) A.F. Henwood, E. Zysman-Colman, Chem. Commun. 53 (2016) 807

[22] Y-J. Yuan, Z-T. Yu, H-L. Gao, Z-G. Zou, C. Zheng, W. Huang, Chem. Eur. J. 19 (2013) 6340

[23] E.C. Stokes, E.E. Langdon-Jones, L.M. Groves, J.A. Platts, P.N. Horton, I.A. Fallis, S.J. Coles, S.J.A. Pope, Dalton Trans. 44 (2015) 8488

[24] J. Hu, M.R. Whittaker, H. Duong, Y. Li, C. Boyer, T.P. Davis, Angew. Chem. Int. Ed. 53 (2014) 7779

[25] (a) K.J. Castor, K.L. Metera, U.M. Tefashe, C.J. Serpell, J. Mauzeroll, H.F. Sleiman, Inorg. Chem. 54 (2015) 6958;

(b) E.E. Langdon-Jones, A.J. Hallett, J.D. Routledge, D.A. Crole, B.D. Ward, J.A. Platts, S.J.A. Pope, Inorg. Chem. 52 (2013) 448.

[26] J. Jayabharathi, R. Sathishkumar, V. Thanikachalam, K. Jayamoorthy, J. Fluoresc. 24 (2014) 445

[27] a) A.D. Becke, J. Chem. Phys. 98 (1993) 5648; b) C. T. Lee, W.T. Yang, R.G. Parr, Phys. Rev. B 37 (1988) 785

[28] Y. Zhao, D. G. Truhlar, Theor. Chem. Acc. 120 (2008) 215

[29] E. V. Ganin, A. E. Masunov, A. V. Siminel, M. S. Fonari, J. Phys. Chem. C 117 (2013) 18154

[30] P. J. Stephens, N. Harada, Chirality 22 (2010) 229

[31] J. Sun, W. Wu, H. Guo, J. Zhao, Eur. J. Inorg. Chem. (2011) 3165

[32] R.O. Bonello, I.R. Morgan, B.R. Yeo, L.E.J. Jones, B.M. Kariuki, I.A. Fallis, S.J.A. Pope, J. Organomet. Chem. 749 (2014) 150.

[33] C. Jin, J. Liu, Y. Chen, L. Zeng, R. Guan, C. Ouyang, L. Ji, H. Chao, Chem. Eur. J. 21 (2015) 12000

[34] S. Lamansky, P. Djurovich, D. Murphy, F. Abdel-Razzaq, H-E. Lee, C. Adachi, P.E. Burrows, S.R. Forrest, M.E. Thompson, J. Am. Chem. Soc. 123 (2001) 4304.

[35] M. J. Frisch, G. W. Trucks, H. B. Schlegel, G. E. Scuseria, M. A. Robb, J.R. Cheeseman, G. Scalmani, V. Barone, B. Mennucci, G. A. Petersson, H. Nakatsuji, M. Caricato, X. Li, H. P. Hratchian, A. F. Izmaylov, J. Bloino, G. Zheng, J. L. Sonnenberg, M. Hada, M. Ehara, K. Toyota, R. Fukuda, J. Hasegawa, M. Ishida, T. Nakajima, Y. Honda, O. Kitao, H. Nakai, T. Vreven, J. A. Montgomery Jr, J. E. Peralta, F. Ogliaro, M. Bearpark, J. J. Heyd, E. Brothers, K. N. Kudin, V. N. Staroverov, T. Keith, R. Kobayashi, J. Normand, K. Raghavachari, A. Rendell, J. C. Burant, S. S. Iyengar, J. Tomasi, M. Cossi, N. Rega, J. M. Millam, M. Klene, J. E. Knox, J. B. Cross, V. Bakken, C. Adamo, J. Jaramillo, R. Gomperts, R. E. Stratmann, O. Yazyev, A. J. Austin, R. Cammi, C. Pomelli, J. W. Ochterski, R. L. Martin, K. Morokuma, V. G. Zakrzewski, G. A. Voth, P. Salvador, J. J. Dannenberg, S. Dapprich, A. D. Daniels, O. Farkas, J. B.

Foresman, J. V. Ortiz, J. Cioslowski, D. J. Fox, Gaussian 09, Revision C.01; Gaussian Inc.: Wallingford CT, 2010.

[36] T. Yanai, D. P. Tew, N. C. Handy, Chem. Phys. Lett. 393 (2004) 51

[37] S. Grimme, J. Antony, S. Ehrlich, H. Krieg, J. Chem. Phys. 132 (2010) 154104.

[38] a) D. Andrae, U. Haussermann, M. Dolg, H. Stoll, H. Preuss, Theor. Chim. Acta 77 (1990) 123; b) T. H. Dunning Jr. J. Chem. Phys. 90 (1989) 1007.

[39] A. Vlček, S. Zalis, Coord. Chem. Rev. 251 (2007) 258

[40] J. Tomasi, B. Mennucci, R. Cammi, Chem. Rev. 105 (2005) 2999.

[41] a) M. Frank, M. Nieger, F. Vogtle, P. Belser, A. von Zelewsky, L. de Cola, V. Balzani, F. Barigelletti, L. Flamigni, Inorg. Chim. Acta 242 (1996) 281; b) A. Juris, V. Balzani, F. Barigelletti, S. Campagna, P. Belser, A. von Zelewsky, Coord. Chem. Rev. 84 (1988) 85.

[42] N.M. Shavaleev, H. Adams, J.A. Weinstein, Inorg. Chim. Acta 360 (2007) 700.

[43] M. Nonoyama, Bull. Chem. Soc. Jpn. 47 (1974) 767